Polymer Chemistry

Accepted Manuscript

This is an *Accepted Manuscript*, which has been through the Royal Society of Chemistry peer review process and has been accepted for publication.

Accepted Manuscripts are published online shortly after acceptance, before technical editing, formatting and proof reading. Using this free service, authors can make their results available to the community, in citable form, before we publish the edited article. We will replace this *Accepted Manuscript* with the edited and formatted *Advance Article* as soon as it is available.

You can find more information about *Accepted Manuscripts* in the Information for Authors.

Please note that technical editing may introduce minor changes to the text and/or graphics, which may alter content. The journal's standard Terms & Conditions and the Ethical guidelines still apply. In no event shall the Royal Society of Chemistry be held responsible for any errors or omissions in this *Accepted Manuscript* or any consequences arising from the use of any information it contains.

ROYAL SOCIETY OF CHEMISTRY

www.rsc.org/polymers

Aggregation Enhanced Excimer Emission (AEEE) with Efficient Blue Emission Based on Pyrene Dendrimers

Alaa S. Abd-El-Aziz,* Amani A. Abdelghani, Brian D. Wagner, and Elsayed M. Abdelrehim

Department of Chemistry, University of Prince Edward Island, 550 University Avenue, Charlottetown, PE, C1A 4P3, Canada

*Corresponding Author E-mail: abdelaziz@upei.ca

Abstract

Fluorescence dendrimers have been developed, which exhibit aggregation enhanced excimer emission (AEEE). In this article, the synthesis and characterization of three generations of organoiron dendrimers with a flexible core is described. Different photoactive pyrene moieties with and without alkyl chains were used to functionalize the dendritic peripheries. The luminescence properties of these dendrimers were examined in various solvents and concentrations as well as in THF/water mixtures. It was determined that the alkyl chain attached to pyrene moieties had a significant impact on the emission wavelength. Interestingly, dendrimers exhibited weak emission when dissolved in organic solvents but strong emission when aggregated in mixed organic/aqueous solvents. Different emission behaviour was observed in the case of second generation dendrimer, due to the presence of a high number of pyrene moieties. The solution emitted much bluer light relative to the zero and first generations, which emitted around 480 nm. In addition, the change in the distance between two pyrene moieties affects the formation of strong or weak excimers. The

excimer-monomer intensity ratios (I_E/I_M) showed the existence of the unique phenomenon of AEEE. The large difference between the aggregated molecules in various THF/water ratios was detected by TEM. Redox activities of the dendrimers were also measured. A single redox wave was displayed in all dendrimers and the intensity of the redox waves increased by increasing the dendrimer generation. All dendrimers possessed good thermal stability and were shown to have two thermal degradation processes.

Keywords: Dendrimer, Pyrene, Fluorescence, Organoiron, Redox-active, Dynamic excimer, Static excimer, Inter- intramolecular π-stacking interaction, TEM, SEM.

1. Introduction

Over the past few years the discovery of a new class of distinct macromolecules which have highly branched molecular architectures, known as dendrimers, has received tremendous interest in light of their potential catalytic, redox, photo- and biological activities.[1-4] Dendrimers display more consistent structures, with a globular shape and a specific molecular weight, than traditional linear polymers.[5] The high level of control available over the design of dendrimers, due to their size, configuration, branching length, and their surface functionality, makes them unique and useful for many applications.[6] Researchers are now focusing on modification of the properties of dendritic molecules by changing the peripheral functional groups of the dendrimer.[4] These dendrimers present potential applications in many fields such as drug delivery, solar cells, catalysis, and electrochemical sensors. Two well-documented approaches used to synthesize dendrimers are the divergent approach reported by Tomalia *et* al.[2] and Newkome et al.,[3] and the convergent approach reported by Hawker and Fréchet.[7, 8] Lately, attention has shifted towards building dendrimers containing metal

groups in their center, branches, or periphery.[9-12] The interest in introducing metal complexes into dendritic structures is to allow access to highly-ordered structures with attractive magnetic, electronic, photo-optical properties, and bioactivity.[13] In particular, the incorporation of organo-transition metal moieties within dendritic structures is a target of great interest in both organometallic and dendrimer research, in order to open up a new family of organometallic macromolecules with many unique properties.[13] This is especially noted for the transition-metal sandwich complexes due to the stereoelectronic characteristics of the delocalized π-cyclic ring ligands.[14-17] The presence of several equivalent, noninteracting redox-active units provides the simultaneous exchange of a large number of electrons that accentuate the electron transfer rate.[18] Moreover, our research group has been focused on the use of η^6-aryl-η^5-cyclopentadienyliron (II) in many classes of macromolecules that involve linear polymers,[19] star polymers[20] dendrimers,[12] and hyper-branched polymers.[21] Dendrimers that contain a photo- and/or electroactive species, in the core or in the dendritic branches, are particularly interesting due to their capability of performing many functions (e.g., photochemical and electrochemical properties).[22-25] It is worth noting that the photochemical and photophysical properties of dendrimers are especially exciting, as the interaction between the photoactive components can result in dendrimers with potentially useful properties.[18] In addition, the presence of luminescence signals can give valuable information to better understand the dendritic structure,[18] and represent possible components for fluorescence-based sensor development. Pyrene is an important polycyclic aromatic fluorescent molecule which is widely used as a fluorescent probe, because of its unique properties, such as a relatively long singlet lifetime and well-defined vibrionic emission bands which are highly sensitive to solvent.[26] Upon photoexcitation, π-stacking interactions between two pyrene molecules in the ground state (static) or in the excited state (dynamic) may result in excimer emission, *i.e.* the appearance of a new emission band, red-shifted with

respect to the usual monomer emission band.[27-29] Commonly, pyrene molecules in the ground and/or excited states inter- or intra-molecularly stack to form excimers and the wavelength corresponding to the maximum of excimer emission (λ_E) for pyrene is typically located at 465-485 nm.[26] An excimer is defined as a pair of pyrene units that, in the ground state, are joined together only weakly (in solid states) or not bonded (in solution). This excimer absorbs light as monomers and emits it in the excited state as a dimer.[27] The excimer emission wavelength of pyrene in solution has been shown to be extremely sensitive to the polarity of the solvent and the concentration of pyrene.[30] The pyrene excimer is suggested to have a symmetrical sandwich-like structure and its emission is red-shifted relative to the monomer emission.[31] The change in fluorescence emission intensity ratios between the pyrene excimer and monomer (I_E/I_M) and the wavelength of maximum excimer emission (λ_E) are two informational parameters connected with the pyrene excimer. Birks and coworkers studied the excimer formation in detail.[32] According to Birks, two pyrene units create an excimer when one monomer in the excited-state comes in close vicinity to another monomer in ground state, and this type of excimer is referred to a ‘‘dynamic excimer’’.[33] The second type of excimer is called a ‘‘static excimer’’ resulting from the excitation of a pyrene dimer in the ground state.[33, 34] Chromophoric organics are often strongly emissive when dissolved in dilute solutions of suitable solvents, but become weakly luminescent when aggregated in poorly solubilizing solvents or in the solid state and this phenomenon is defined as aggregation quenching emission (AQE).[35, 36] However, an opposite phenomenon was discovered in 2001 called aggregation-induced emission (AIE), in which luminescent materials which are weakly emissive in solution become stronger emitters in an aggregated phase.[37, 38] In the aggregation, the pyrene molecules are located in the immediate vicinity of each other and undergo strong intermolecular interactions, which cause the formation of species such as excimers and exciplexes that contribute to new luminescence bands. Furthermore, aggregation enables

dynamic intermolecular charge transfer[39] and can positively restrict the intramolecular rotation (RIMR) of the fluorophores.[40, 41] Consequently, this excimer emission can also be used indirectly to identify the aggregation process of pyrene derivatives.[42] Furthermore, interplay distance between two pyrenes may change at the interface between the ends of two aggregates, and some of these local geometries may be fitting for excimer formation after photoexcitation.

Continuing work in the field of photoactive, organometallic dendrimers,[43, 44] we report herein new fluorescent dendrimers with a flexible core. In these dendrimers, we utilized pyrene to functionalize the zero, first and second generation for the construction of new luminogens and investigated their photophysical properties. We have also examined the fluorescence properties and excimer formation of aggregated dendrimers in THF/water mixtures. The emission intensities of excimer-monomer ratio (I_E/I_M) were investigated. TEM has been used to detect aggregation states of the dendrimers which showed a huge difference in particle size, shape, and distribution in various water fractions. In addition, the electrochemical behaviors and thermal stabilities of these complexes were examined.

2. Experimental

2.1 Materials

All chemicals and reagents were obtained from Sigma-Aldrich and were used without any further purification. All solvents were dried and stored over 3 Å molecular sieves before being used. The synthesis of the organoiron complexes **5, 7,** and **9** followed previously reported procedures.[19, 45, 46]

2.2 Instrumentation

A Bruker Avance NMR spectrometer (^{1}H, 300 MHz and ^{13}C, 75 MHz) was used to characterize all synthesized complexes in DMSO-d_6 or Acetone-d_6 with the chemical signals referenced to solvent residual signal in ppm. Attenuated total reflection Fourier transform IR (ATR-FTIR) absorption spectroscopic measurements were acquired on a Bruker Alpha FTIR spectrometer Alpha-P. Cyclic voltammetric experiments were carried out on a Princeton Applied Research/EG&G Model 263 potentiostat/ galvanostat using glassy carbon working electrode, Pt counter electrode, and Ag reference electrode. The experiments, which were carried out at a scan rate between 0.1 and 1.5Vs^{-1} and at a temperature between 25^{o}C and -25°C under nitrogen atmosphere in degassed propylene carbonate as solvent and tetrabutylammonium hexafluorophosphate as supporting electrolyte, were externally referenced to a DMF solution of ferrocene. The scanning electron micrographs (SEM) of the complexes were obtained on a Hitachi TM3000 SEM. Transmission Electron Microscope (TEM) Hitachi Bio TEM 7500 Electron microscope was operated at 80 kV. Images were captured with a side mounted digital camera AMT XR40, bought from Advance Microscopy Techniques, Danvers, MA, USA. Grids used in the experiment were 200 mesh copper grids carbon coated acquired from SPI Supplies Canada, London Ont. Elemental analyses were performed on CE-440 Elemental Analyser, Exeter Analytical, Inc. Thermogravimetric analysis (TGA) was conducted in platinum pans under nitrogen at a heating rate of 10°C on a TA Instruments TGA Q500. Fluorescence data were acquired on Photon Technology International Quantum Master 400

spectrofluorimeter. UV-vis absorption measurements were performed using a HP8543 UV-vis spectrophotometer.

2.3 Synthesis and characterization

General procedures

Steglich esterification[47] was used to synthesize compounds **2a**, and **3a** by using 1:1 molar ratio of reactants as described in detail in the supplementary information. The solutions were stirred at 0°C under nitrogen atmosphere. The reaction mixtures were then stirred under nitrogen for 24 hours at room temperature. The reaction mixtures were cooled to -25°C in a freezer for two hours, filtered to remove dicyclohexylurea (DCU) and then poured into 10% HCl solution. The products were extracted with three times with 50 mL DCM, washed with 100 mL portions of water five times, then dried over $MgSO_4$, filtered, and the solvent removed with a rotary evaporator. The products were dissolved in acetone, cooled to –25°C in a freezer for two hours, filtered to remove remaining DCU and removal of the solvent gave rise to the products. The same methodology was used to synthesize dendrimers **D2a**,**b**, **D4**, and **D6** by using 1:4 molar ratio, to synthesize dendrimers **D8** and **D10** by using 1:8 molar ratio, and **D12** by using 1:16 molar ratio.

Nucleophilic aromatic substitution reactions were used in the synthesis of dendrimer **D1** by using 1:4 molar ratio, **D7** by using 1:8 molar ratio, and **D11** by using 1:16 mmol ratio. The reaction mixtures were stirred in DMF with K_2CO_3 at room temperature between two to three days after flushing with nitrogen for 1/2 hour. Subsequently, the reaction mixtures were poured into 10% HCl solution, and NH_4PF_6

was added to precipitate the products. The products were collected by suction filtration and dried under vacuum at room temperature.

Demetallation procedures followed our previously reported procedure[12, 48] to synthesize dendrimers **D3a,b, D5**, **D9**, and **D13**. The dendrimers were dissolved in acetonitrile in Pyrex test tubes and then flushed with nitrogen for 10 minutes. The mixtures were irradiated with UV radiation for 24 hours in a Rayonett photochemical reactor equipped with 300 nm lamps. The mixtures were then filtered through small silica gel columns and the solvent was evaporated. The residue was extracted with 50 mL chloroform and after that washed with three times 100 mL water. The extracts were dried over $MgSO_4$, followed by evaporation of the chloroform.

Detailed synthetic methodologies for the dendrimers and their precursors, and spectroscopic characterization including ^{1}H and ^{13}C NMR, ATR-FTIR, and elemental analyses data are reported in the Supporting Information.

3. Results and discussion

3.1 Syntheses and characterization of the complexes

Five dendrimers were functionalized with pyrene in zero, first, and second generations, with the redox-active organoiron moieties incorporated throughout every dendritic branch. The diversity among using flexible or rigid arms was designed to study their influence on fluorescence properties. Steglich esterification procedure, interchangeably with nucleophilic aromatic substitution reactions, was used under moderate conditions to synthesize these dendrimers. Three different pyrene derivatives were used to cap dendrimer **D1** in zero generation, after conversion of the carboxylic

group in 1-pyrenbutyric acid **1** to aliphatic alcoholic group (Scheme 1). The divergent synthetic method was used to build the dendrimers from G0 to G2 and an excellent yield was obtained without protection steps. For instance, the synthesis of the zero generation G0 dendrimer **D1**, involved nucleophilic substitution reaction of the Pentaerythritol tetrakis (3-mercaptopropionate) core **4** with complex **5** (Scheme 2). The Steglich esterification procedure was used to synthesize zero generation G0 dendrimers **D2a,b** and **D4** capped with pyrene derivatives. In addition, the successful removal of the organoiron moieties by irradiation with UV lamp formed the organic analogues, dendrimers **D3a,b and D5** (Scheme 3, 4). The same method was also used to synthesize first generation G1 dendrimer **D6** (Scheme 5). The nucleophilic substitution reaction of the latter with 4-hydroxybenzyl alcohol **8** was used to form more functionalized first generation G1 dendrimer **D7** (Scheme 6). The first generation G1 dendrimers **D8** and **D9** were decorated with pyrene through using Steglich esterification procedure followed by irradiation with a UV lamp (Scheme 7). Second generation G2 followed the divergent synthetic route to form second dendrimer **D10** (Scheme 8). 4-hydroxybenzyl alcohol **8** reacted with dendrimer **D10** to form dendrimer **D11** through nucleophilic substitution reaction (Scheme 9). Dendrimer **D12** capped with pyrene also followed Steglich esterification procedure, followed by irradiation with a UV lamp to form dendrimer **D13** (Scheme 10). It is important to note that the nucleophilic substitution reactions were carried out under mild conditions due to the activation of the cyclopentadienyliron moieties.

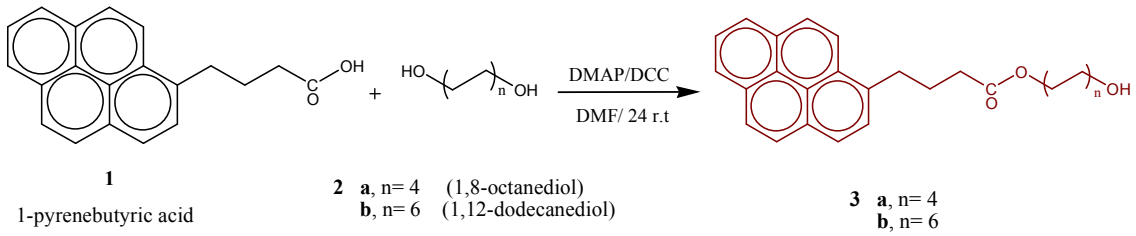

1
1-pyrenebutyric acid

2 **a**, n= 4 (1,8-octanediol)
b, n= 6 (1,12-dodecanediol)

3 **a**, n= 4
b, n= 6

Scheme 1. Synthesis of alcoholic long chain pyrene **3a** and **3b**

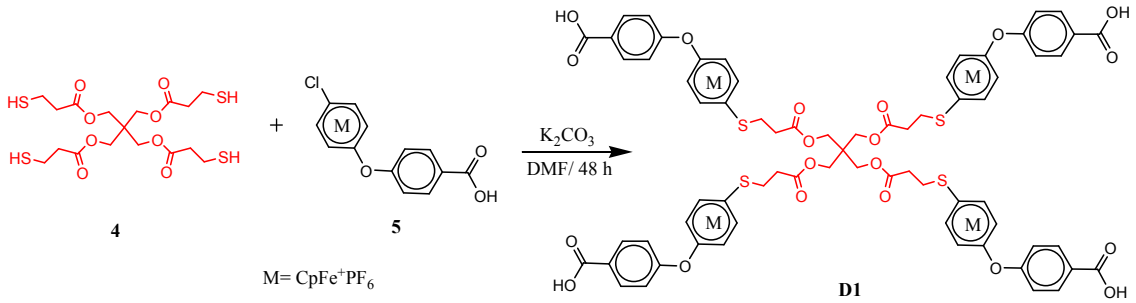

4

5

M= $CpFe^{+}PF_6$

D1

Scheme 2. Synthesis of dendrimer **D1**.

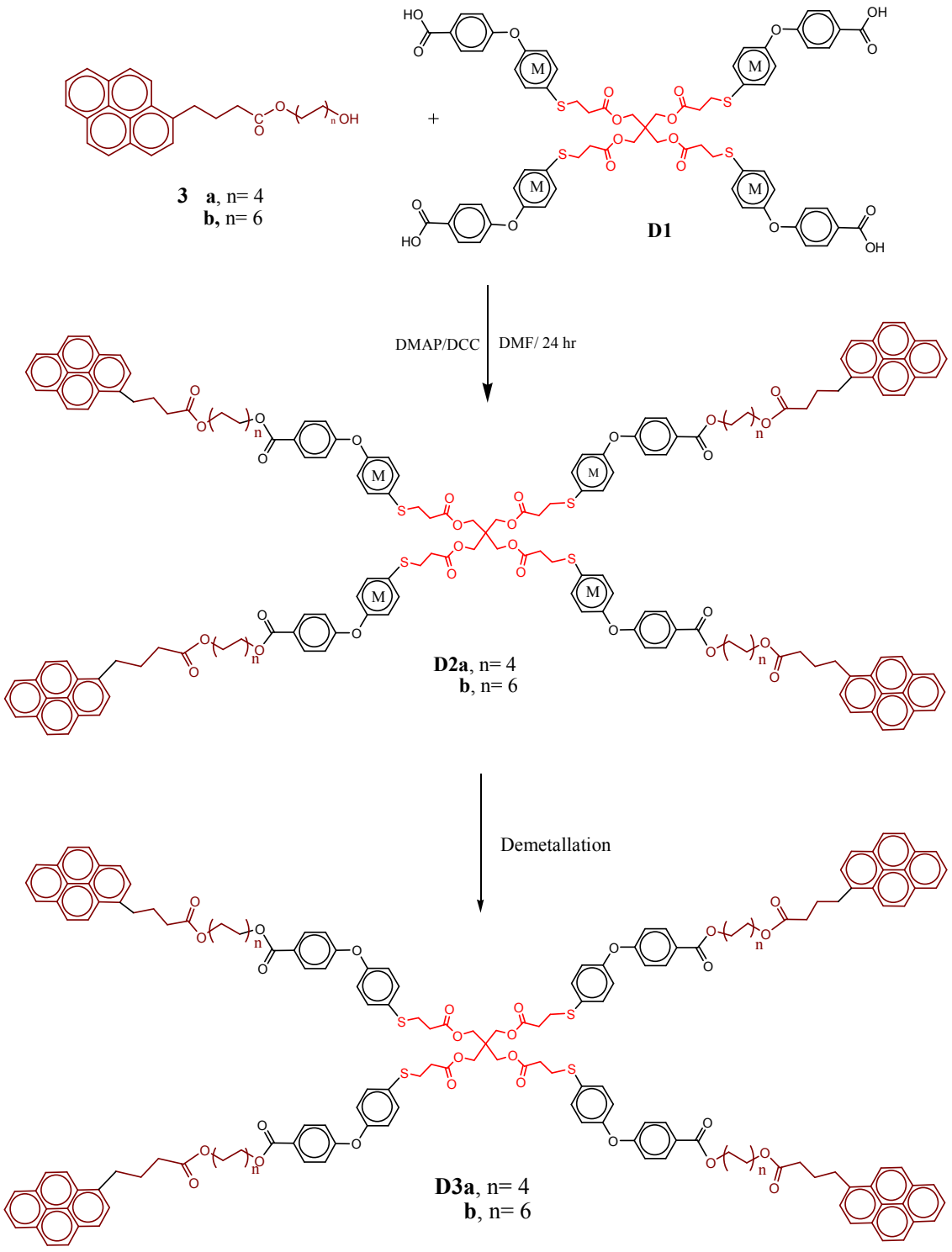

Scheme 3. Synthesis of dendrimer **D2a, b** and **D3a, b**.

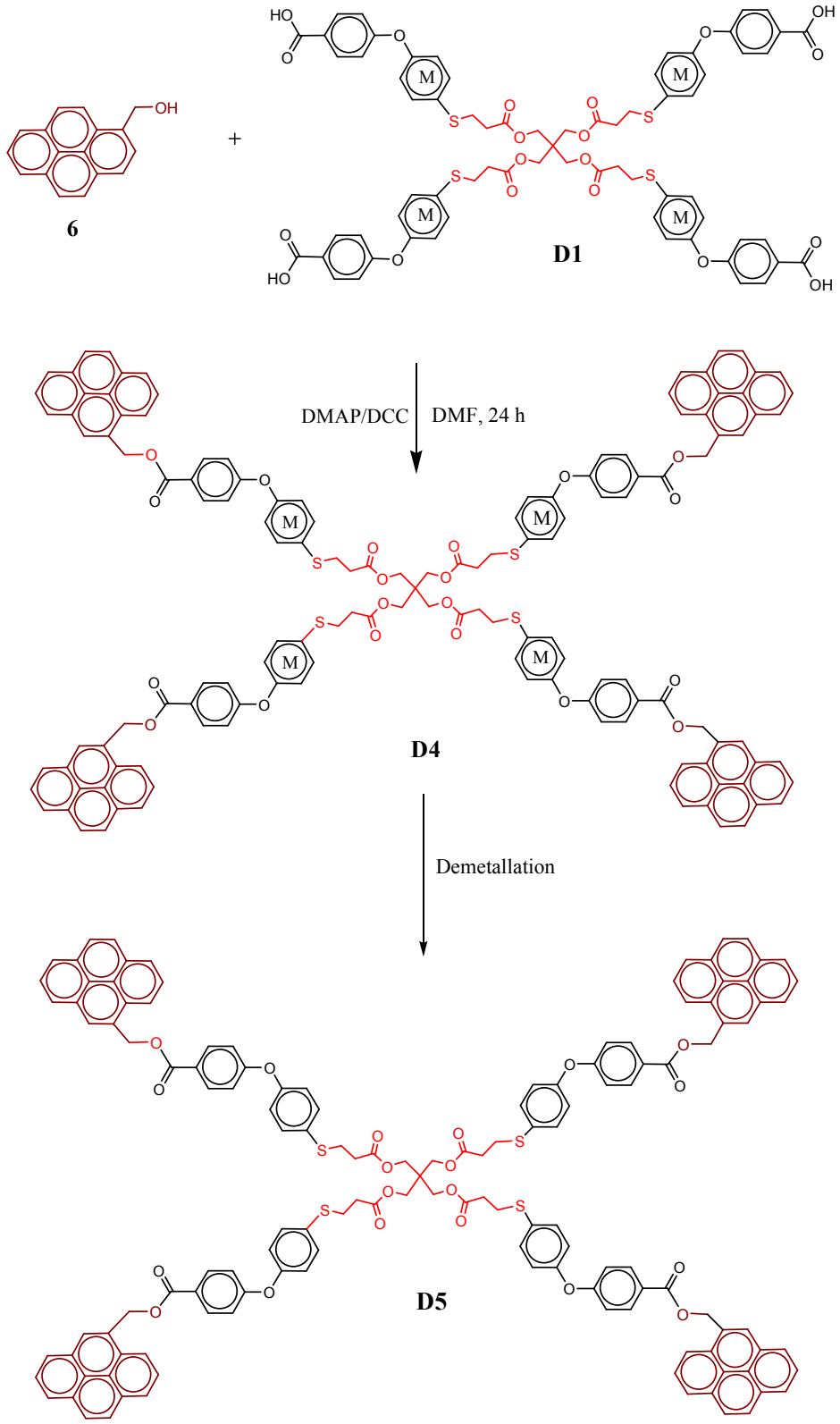

Scheme 4. Synthesis of dendrimer **D4** and **D5**.

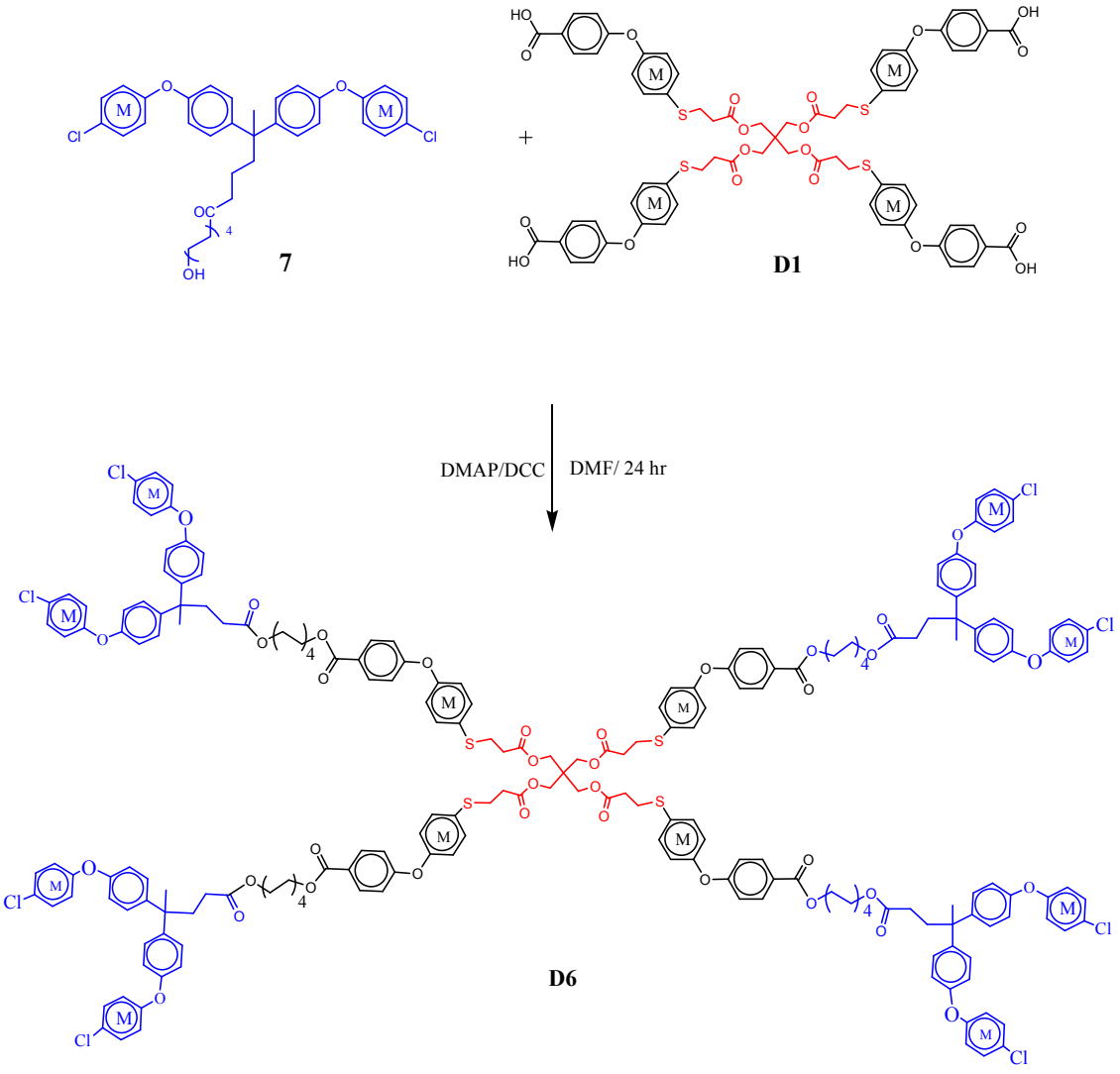

Scheme 5. Synthesis of dendrimer **D6**

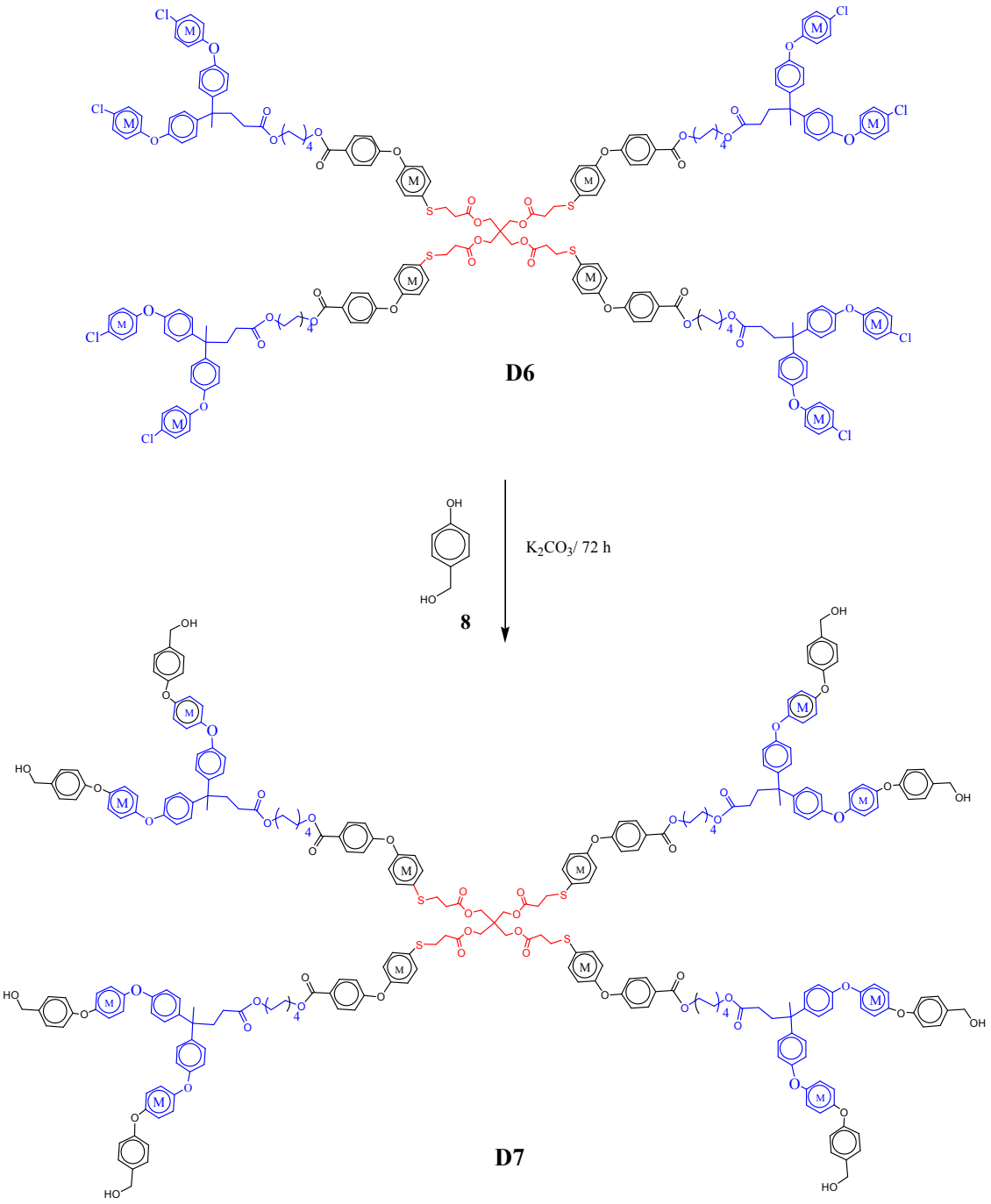

Scheme 6. Synthesis of dendrimer **D7**

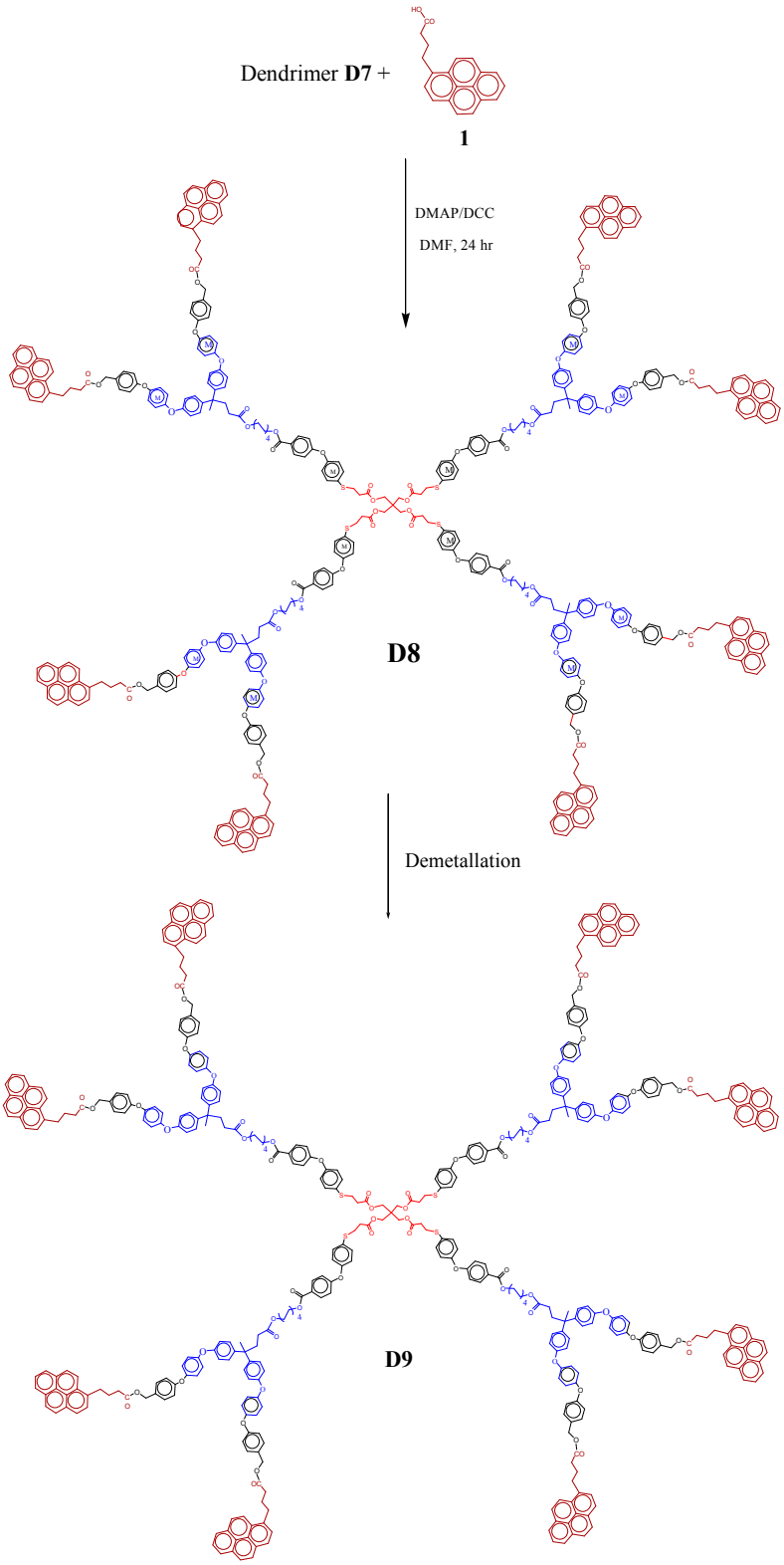

Scheme 7. Synthesis of dendrimer **D8** and **D9**.

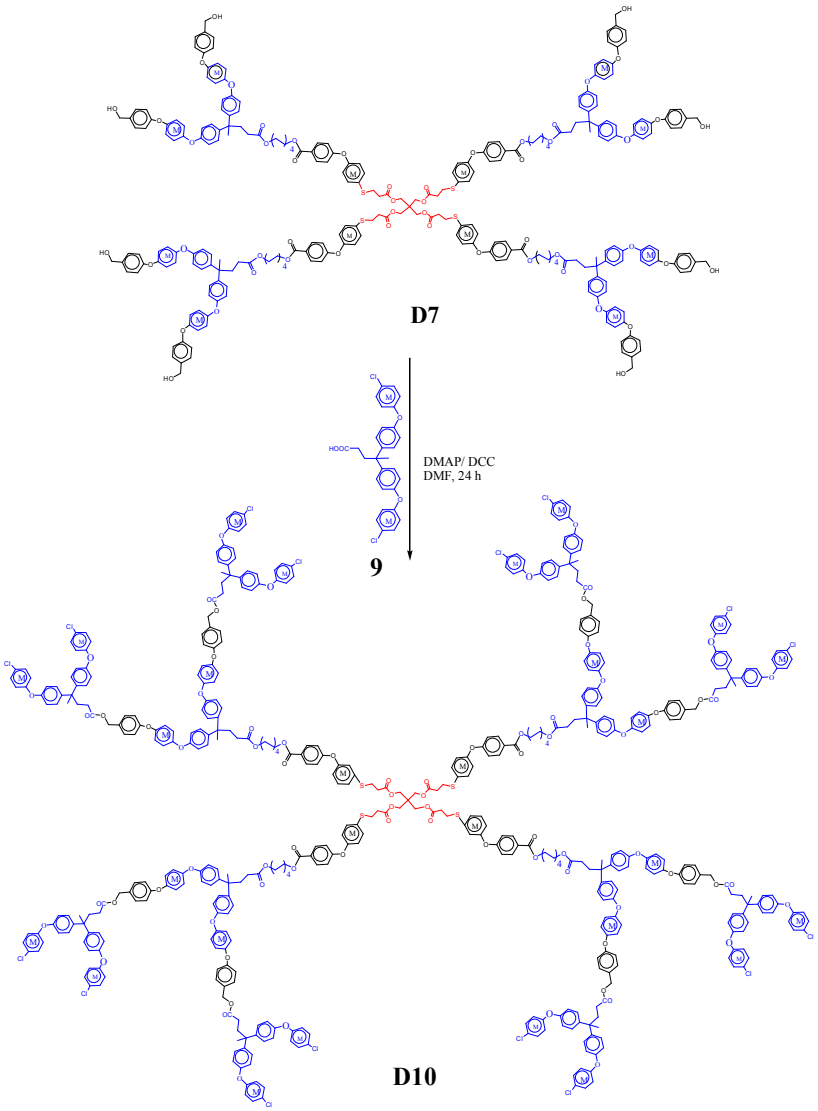

Scheme 8. Synthesis of dendrimer **D10**

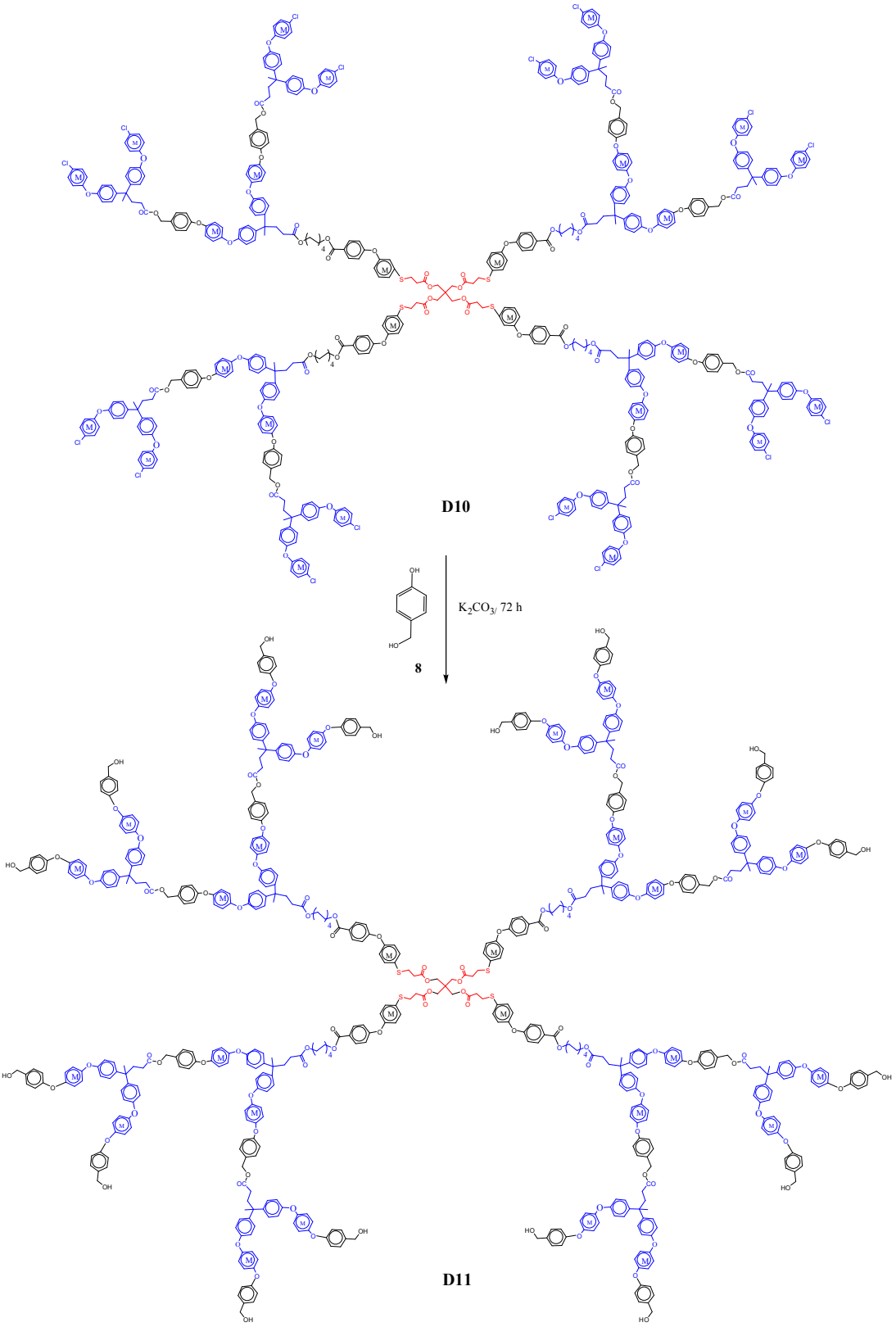

Scheme 9. Synthesis of dendrimer **D11**

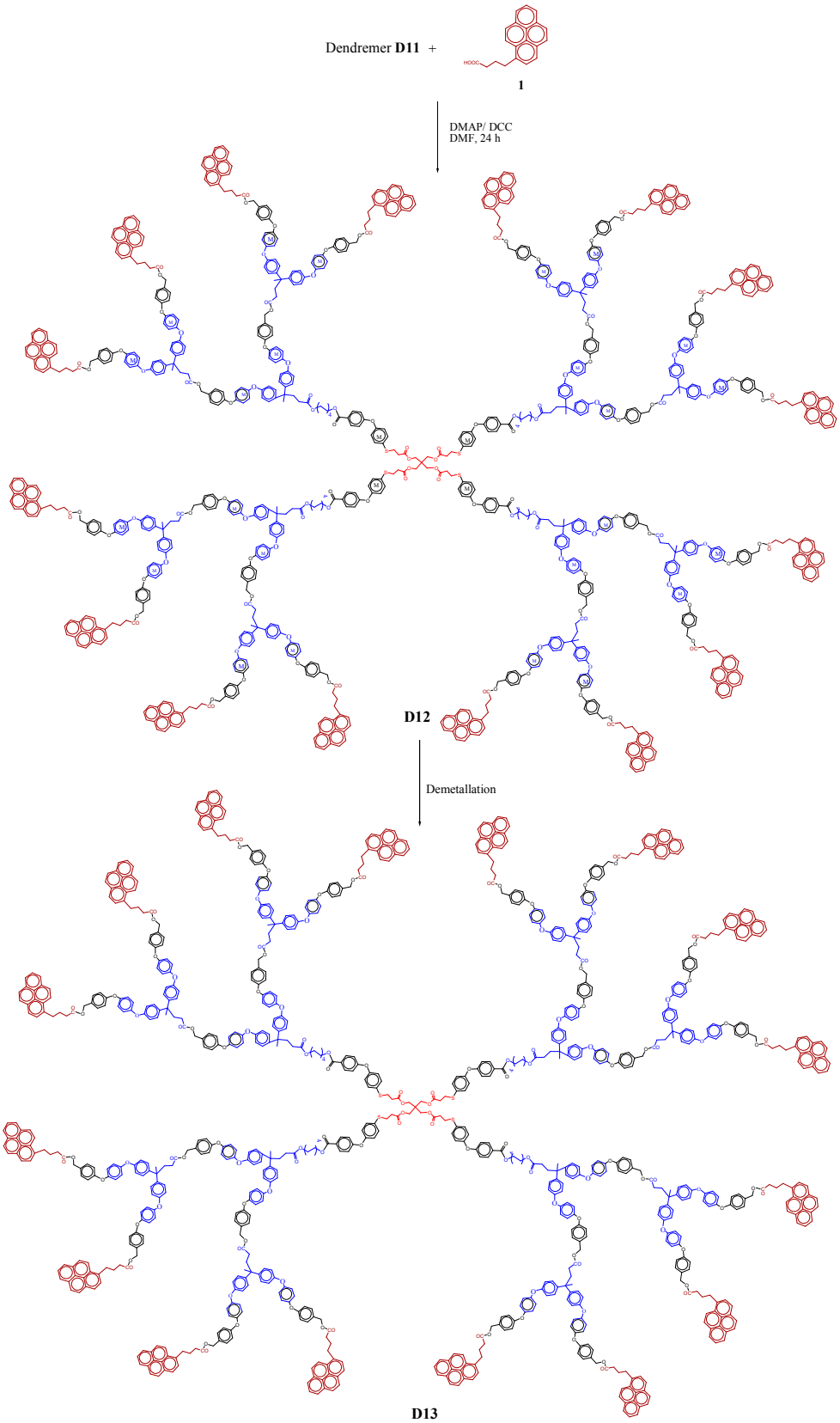

Scheme 10. Synthesis of dendrimer **D12** and **D13.**

^{1}H and ^{13}C NMR, IR as well as elemental analysis were used to characterize and confirm the synthesized dendrimers. The shift in ^{1}H NMR peaks of these dendrimers supported their successful syntheses. For instance, zero generation dendrimer **D1** showed one signal at 6.49 ppm, which refers to 16 protons in the four complexed aryl groups. Moving to the first generation dendrimer **D6**, two distinct peaks appeared at 6.82 and 6.44 ppm, the first one shifted downfield indicating outer complexed aryl groups attached to the peripheral chloro- end group. The second one refers to the complexed aryl groups attached to the etheric oxygen groups. On peripheral functionalization of dendrimer **D6** with 4-hydroxybenzyl alcohol to yield dendrimer **D7**, these complexed protons resonated upfield at 6.26 ppm as one peak due to equivalent surrounding etheric oxygen groups. Furthermore, in the second-generation dendrimer **D10**, the protons of the inner complexed aryl groups appeared at 6.27 ppm, clearly differentiated from those of the outer complexed aryl groups which resonated at two different frequencies 6.44 and 6.81 ppm, due to non-equivalent attached groups. Broadening of the peaks was observed with increasing generation of dendrimers, as expected,[12, 49] and the peak intensities integrated consistently with the number of protons. Additionally, in zero generation dendrimer **D1**, one peak at 5.18 ppm that corresponded to the protons of the Cps was observed, whereas in dendrimer **D6** two peaks appeared at 5.28 and 5.15 ppm that corresponded to the protons of the two distinct Cps. These two Cp peaks of dendrimer **D6** became one peak resonating at 5.22 ppm in dendrimer **D7**. This peak appeared due to the equivalence of the surrounding groups at the *para* positions. By addition of the 1-pyrene butyric acid, the ^{1}H NMR showed two Cp peaks due to the presence of pyrene moieties as seen in Figure 1 (due to the large scale of the dendrimers, we drew only one arm in the figure for illustration). Moreover, the ^{1}H NMR spectrum of dendrimer **D10** also shows two Cp

peaks with integration in agreement with the ratio of Cp protons in the periphery attached either to chloro-arenes or to those in the inner attached to etheric oxygen groups. The integration of the signals indicates which peak represents the inner and which one the outer Cp groups. The carboxylic groups in dendrimer **D1** which resonate at 13.16 ppm disappeared due to the formation of the ester groups. The OH groups of the 4-hydroxybenzyl alcohol substituents appeared at 4.37 ppm in the first generation dendrimer **D7** which disappeared in the second generation dendrimer **D10** due to the formation of the ester linkage.

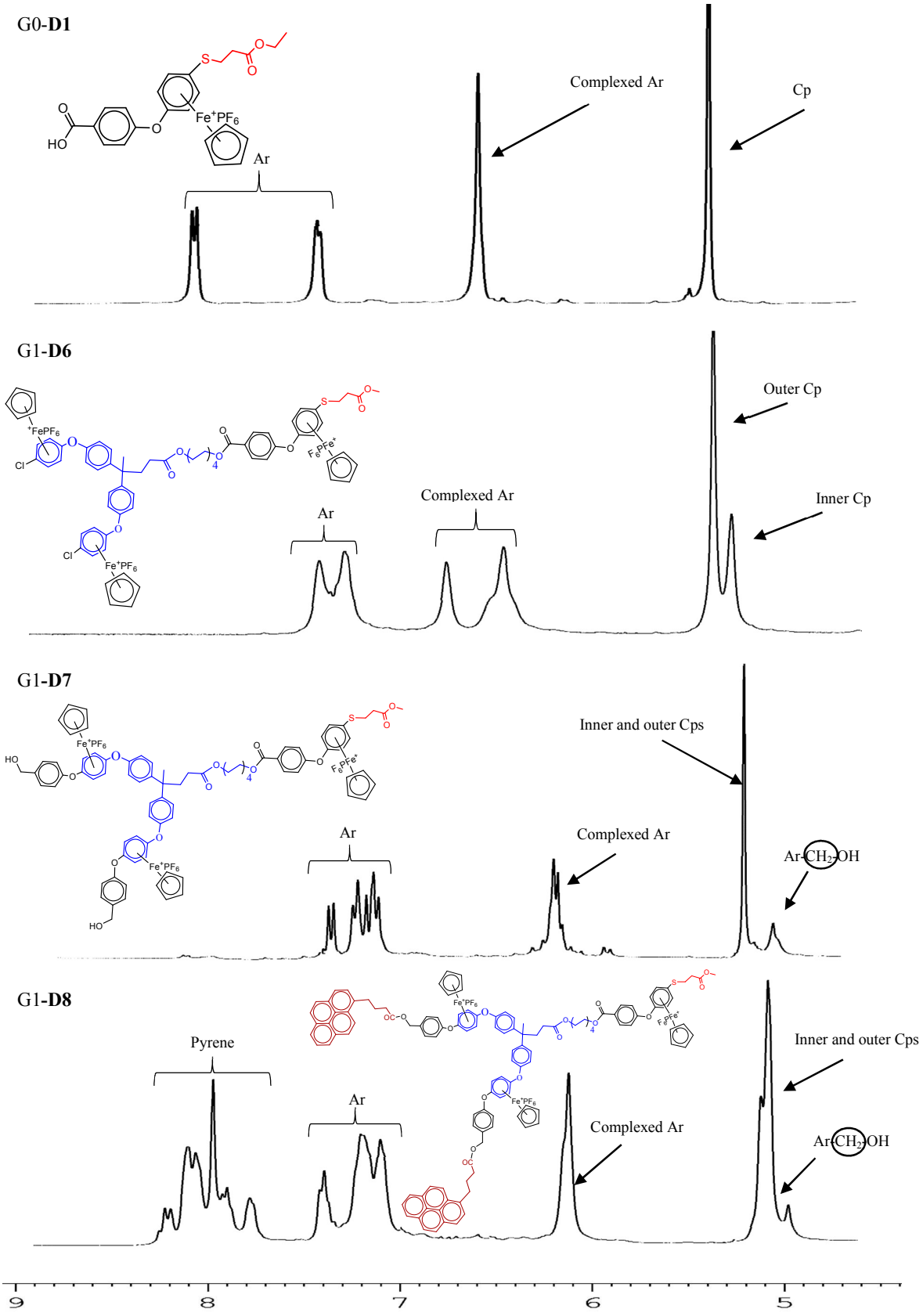

Figure 1. ^{1}H NMR spectra for **D1**, **D6**, **D7**, and **D8**.

Successful syntheses of these dendrimers were also confirmed by ^{13}C NMR spectroscopy. For example, carbonyl groups showed two peaks at 171.51 and 167.35 ppm for the zero generation dendrimer **D1**. Three peaks appeared in the spectrum of dendrimer **D2a** at 173.69, 171.54 and 167.35 ppm due to the three carbonyl groups. It was expected that more than three carbonyl peaks in the second generation would appear, however, just three peaks were observed. The peak at 173.76 ppm was attributed to overlapped peaks of the carbonyl carbons of the two outer ester linkages. Similarly, one peak in the zero generation dendrimers **D1**, **D2a,b,** and **D4** corresponded to the Cp carbons around 78.50 ppm. Two distinct Cp carbon peaks around 80.23 and 79.69 ppm, appeared in the first generation, which confirms the formation of this generation. Furthermore, in the presence of the peripheral chloro-end group, the complexed CH aromatics resonate at around 87.50 and 76.50 ppm, while the complexed CH aromatics with ester linkages resonate at around 78.50 and 76.50 ppm. Uncomplexed carbons resonate around 130.00 ppm and quaternary carbons were detected around 122.80 ppm. The carbon of $ArCH_2O$ was detected around 63 ppm. As we have observed in the ^{1}H NMR of higher generation dendrimers, the ^{13}C NMR also exhibited overlapped peaks.

The demetallation of dendrimer **D3a,b**, **D5**, **D9**, and **D13** was successfully completed resulting in the complete removal of the Cp peak, which disappeared in the ^{1}H NMR and ^{13}C NMR spectra. In addition, a downfield shift occurred for the complexed aromatic protons to the region of uncomplexed aromatic protons due to the removal of FeCp as shown in Figure 2.

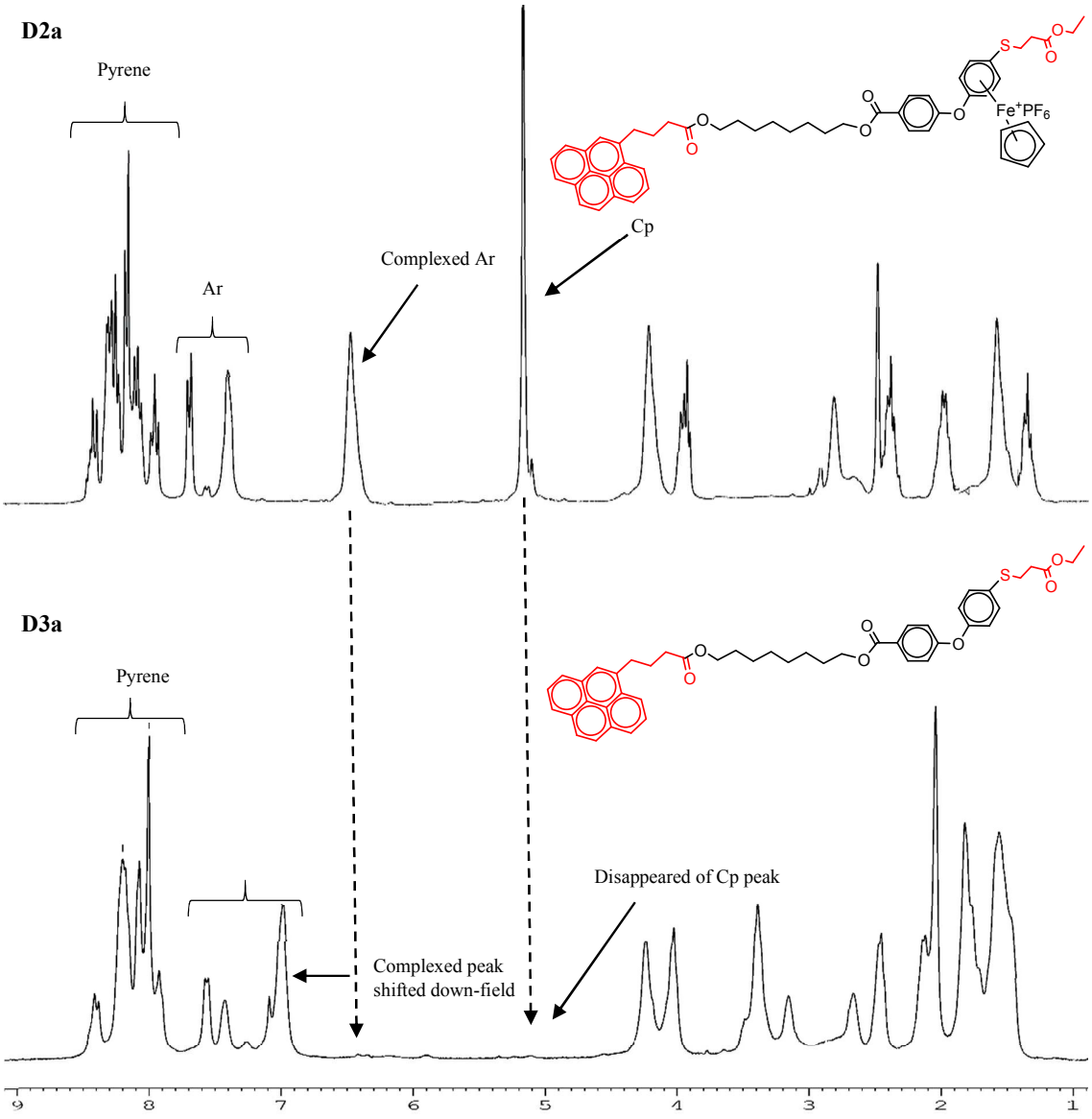

Figure 2. ^{1}H NMR spectra of **D2a** and demetallated **D3a**

The ATR-FTIR absorption spectra showed the presence and characteristic bands of hydroxyl, ester and ether groups, respectively, around 3300, 1700 and 1220 cm^{-1}. Elemental analysis has further confirmed the dendrimers' formation as outlined in the experimental section.

In addition, the surface morphology of dendrimers **D1**-G0, **D6**-G1, and **D10**-G2 were determined by scanning electron microscopy (SEM), to show the difference between each generation. The samples were mounted on a stub of metal with adhesive, coated

with 40-60 nm of gold and then spotted under the microscope. The microscopic images demonstrated the amorphous character of the dendrimers as shown in Figure 3. Zero generation dendrimer **D1** had no particular shape and aggregated as irregular amorphous (Figure 3-a). In the first generation dendrimer **D6,** the particles were seen to have the same shape for the zero generation and strongly aggregated as seen in Figure 3-b. The crystal structure started to appear in the morphology of the second generation dendrimer **D10**, which exhibited an agglomeration of different sizes and shapes. Both the large and small particles have sharp edges (Figure 3-c).

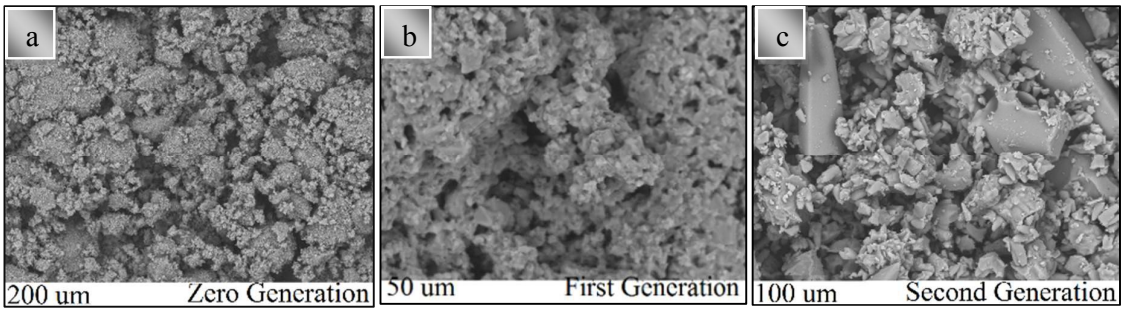

Figure 3. Scanning electron microscope (SEM) images for dendrimers **D1**-a, **D6**-b, **D10**-c.

3.2 Electrochemical properties

Electrochemical properties were studied for all dendrimers at various temperatures between 25^{o}C and -25^{o}C in a solution of 0.1 M Bu_4NPF_6 using a propylene carbonate (as a supporting electrolyte), a Ag/Ag^{+} reference electrode, a glassy carbon working electrode, and a Pt wire counter electrode. The potential was scanned in the range of 0 to -2.0 mV. All these dendrimers contain redox-active η^6-aryl-η^5-cyclopentadienyliron (II) centers in their dendritic arms at every repeated generation to form different redox-active centers, with the number of the redox centers increasing from one generation to the next. All dendrimers in different generations showed a single reversible redox wave, with different intensities dependent on dendrimer generation (Figure 4). At room temperature zero generation

dendrimers **D1, D2a,b,** and **D4** underwent reversible reduction, the average $E_{1/2}$ values is between -1.25 and -1.28 V, and the single redox wave presence in the zero generation is reasonable due to the equivalence of these redox centers.[50, 51] With increasing dendrimer generation, we observed in dendrimer **D6, D7,** and **D8** in the first generation a more negative shift and an increase in intensities in both reduction and oxidation peaks with the broadening of the peaks, as previously reported.[12] This was due to the higher number of cationic irons in both zero and first generation. The average $E_{1/2}$ values were recorded to be between -1.35 and -1.38 V. The more negative shift appeared in the second generation dendrimers **D10, D11,** and **D12** which have 28 redox-active centers with more increase in their redox wave intensities and the average $E_{1/2}$ values were between -1.3 and -1.32 V. The difference in the reduction wave value from zero to second generation is around -1.8 V due to increasing cationic centers. We expected splitting of the redox wave due to the presence of different generation but the speed of electron transfer between the electrodes and iron centers prevent splitting of the redox waves. In addition, overlapped cathodic currents resulted from the reduction of iron centers consistent with our previous studies.[12]

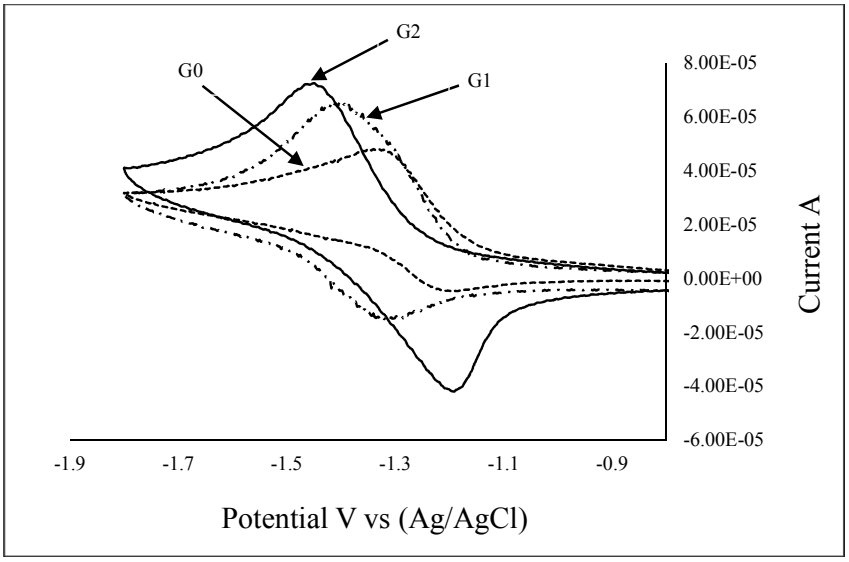

Figure 4. Representative cyclic voltammogram of the generation G0, G1, and G2 in 0.1 M Bu_4NPF_6 in propylene carbonate, scan rate = 200 mV/s, at 25°C

3.3 Thermal analysis

The thermal properties of the cationic organoiron dendrimers were studied using thermogravimetric analysis (TGA) under nitrogen (Figure 5). The first degradation step is ascribed to the loss of the attached cyclopentadienyliron moieties in the dendrimers, which is consistent with previous findings.[12, 52] The three dendrimers exhibited weight loss at slightly different temperatures, 26% weight loss at 208°C for the zero generation (G0), 20% weight loss at 195°C for the first generation (G1), and 18% weight loss at 208°C for the second generation (G2). Large weight losses were exhibited starting between 350°C and 410°C, which were associated with the second degradation step. The second degradation was recorded around 350°C for G0 with 40% weight loss, 375°C for G1 with 62% weight loss, and 410°C for G2 with 65% weight loss, as shown in Figure 5. The increase in the dendrimer generation caused a delay in its second degradation step, illustrating a link between the dendrimer's molecular weight and its thermal stability. At the end of these analyses which was around 510°C, the residual content was around 34.6% for the zero generation and 17.4% for the first and second generations. The higher percentage of residue in the zero generation is due to the higher iron content in this generation relative to the first and second generations.[53]

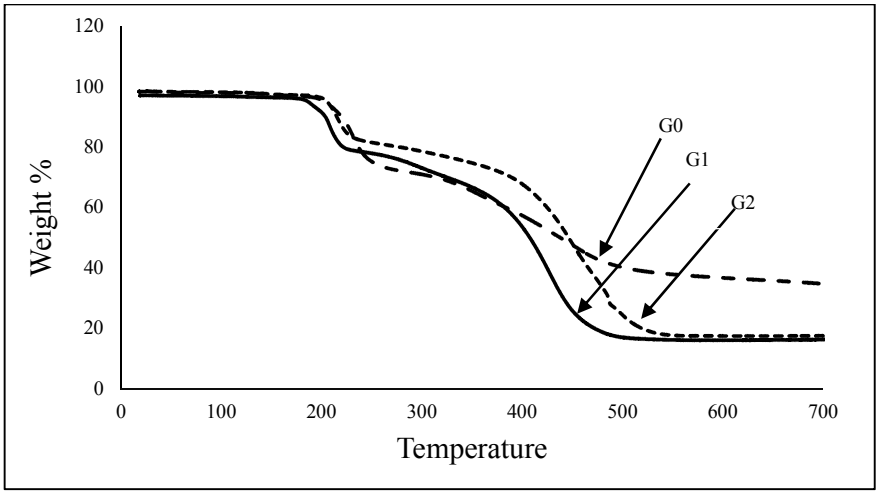

Figure 5. TGA of generations G0, G1, and G2

3.4 Photophysical properties of demetallated dendrimers D3a,b, D5, D9, and D13

With many useful properties and unique structures, dendrimers are very attractive, particularly when they carry a high number of light-absorbing or photoactive chromophores in their peripheries. Pyrene as a useful fluorophore was chosen to cap our synthesized dendrimers to explore the effects of the dendritic structure on their photophysical properties. All three demetallated zero generation dendrimers **D3a,b** and **D5,** and the first generation demetallated dendrimer **D9**, showed almost identical absorption characteristics. The absorption spectra showed no effect of increasing the number of pyrene moieties from four units in the zero generation to eight units in the first generation in the absorption intensities (although an increase was expected). There is a small increase observed in the absorption intensity of the second generation demetallated dendrimer **D13**, due to the higher number of pyrene moieties which have sixteen units in the periphery per molecules with a negligible shift in the absorption range as shown in Figure 6.

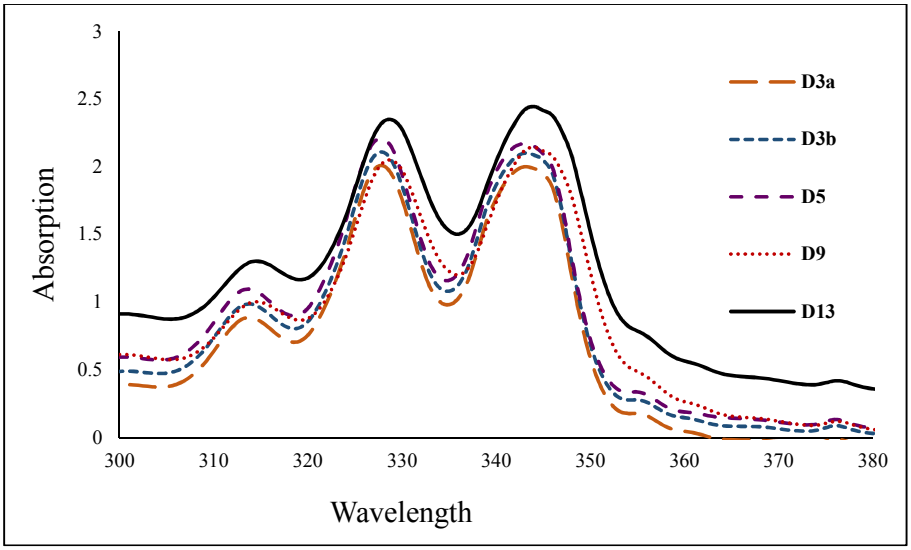

Figure 6. UV-vis absorption spectra of demetallated dendrimers **D3a,b, D5, D9, and D13** (10μM) in THF.

However, there is no effect of the presence or absence of the redox-active iron centers in the shape of the absorption spectra of dendrimers **D2a,b, D4, D8,** and **D12** with organoiron

complexes and demetallated dendrimers **D3a,b, D5, D9,** and **D13** without organoiron complexes as shown in Figure 7, while the intensity of the metallated dendrimers was marginally less than the demetallated version. These results showed that the redox-active iron centers had no significant impact on the absorption band of the chromophoric species, which agrees with findings in previous reports.[54, 55]

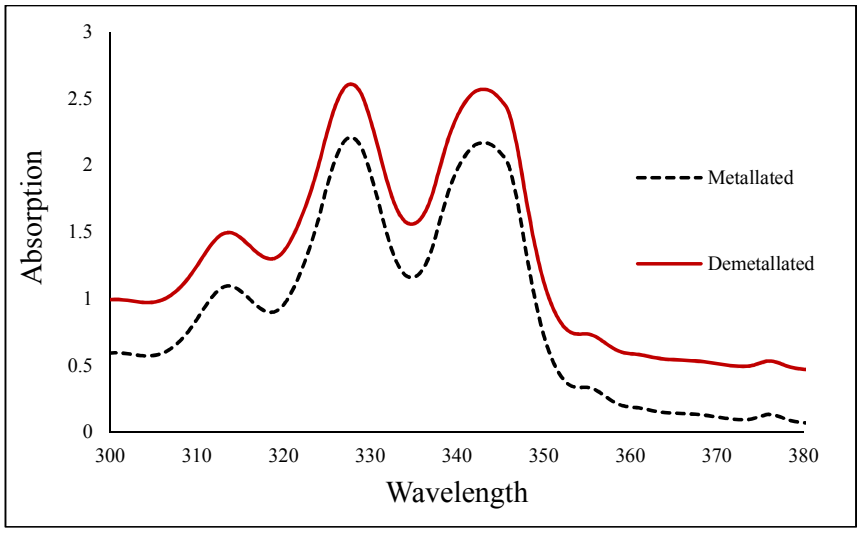

Figure 7. Representative UV-vis absorption spectra of metallated dendrimer **D2a** and demetallated dendrimer **D3a** (10μM) in THF.

The UV-vis spectra of dendrimers **D3a,b, D5, D9,** and **D13** with pyrene moieties in different solvents were found to absorb at 328 and 343 nm as is usual for pyrene derivatives, with similar shape and intensity in every solvent (Figure 8). The maximum wavelength and shape of the absorption spectrum were found to be independent of solvents and characteristic of the monomer, and this indicated that there is no interaction between the two pyrenyl units in the ground state to form dimers.

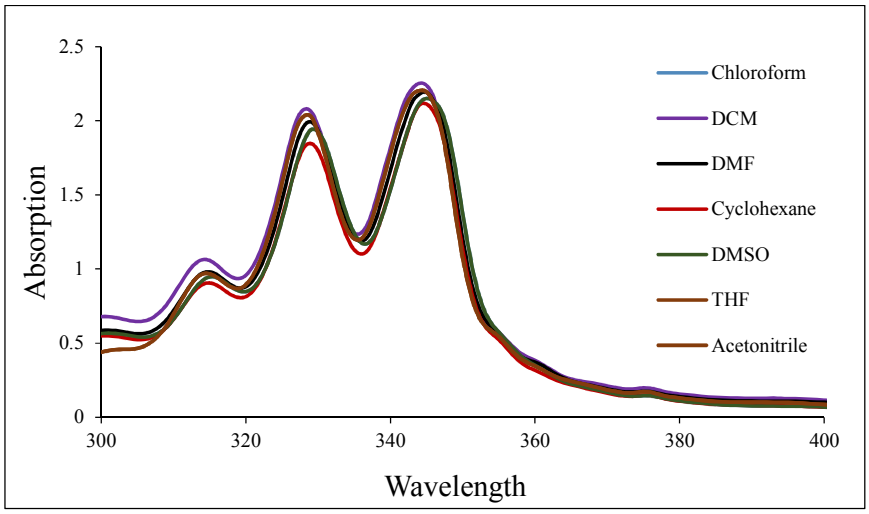

Figure 8. Representative UV-vis absorption spectra of dendrimer **D3a** (10μM) in different solvents.

The fluorescence properties of dendrimers **D3a,b, D5, D9,** and **D13** were examined under different conditions such as the presence and absence of the η^6-aryl-η^5-cyclopentadienyliron (II), varying organic solvents, varying concentrations, and in THF/water solvent mixtures. The aggregation enhanced excimer emission (AEEE) was investigated in THF/water mixtures (from 10:0 to 1:9, v/v). The emission spectrum of dendrimers **D2a,b, D4, D8,** and **D12** with η^6-aryl-η^5-cyclopentadienyliron (II) and pyrene moieties in THF shows typical emission bands at 377 and 398 nm (excitation at λ=343 nm), which were attributed to the pyrene monomeric emission.[56] Thus, the pyrene moieties cannot form a typically observed intramolecular sandwich excimer due to the separation of the two pyrenyl groups by the organoiron complex. This separation leads to either unsuitable distance between two pyrenyl units to form the excimer, or the two pyrenyl units forced to adopt only perpendicular conformation. On the other hand, the spectra of the demetallated dendrimers **D3a,b, D5, D9,** and **D13** showed both the pyrene monomer emission and a red-shift emission typical of pyrene excimer fluorescence,[57] (Figure 9). All demetallated dendrimers exhibited two emissions: a "pyrene monomer" emission due to the spatially separated excited pyrenes, and a "pyrene excimer" emission resulting from the excited-state pairs formed between two

pyrene chromophores upon excitation. The pyrene excimer-monomer ratio (I_E/I_M) was calculated by taking the ratio of the intensity (peak height) of the excimer to the intensity of the monomers. The excimer wavelength and the excimer-monomer ratio were different depending on the dendrimer generation and the flexibility of the structure.

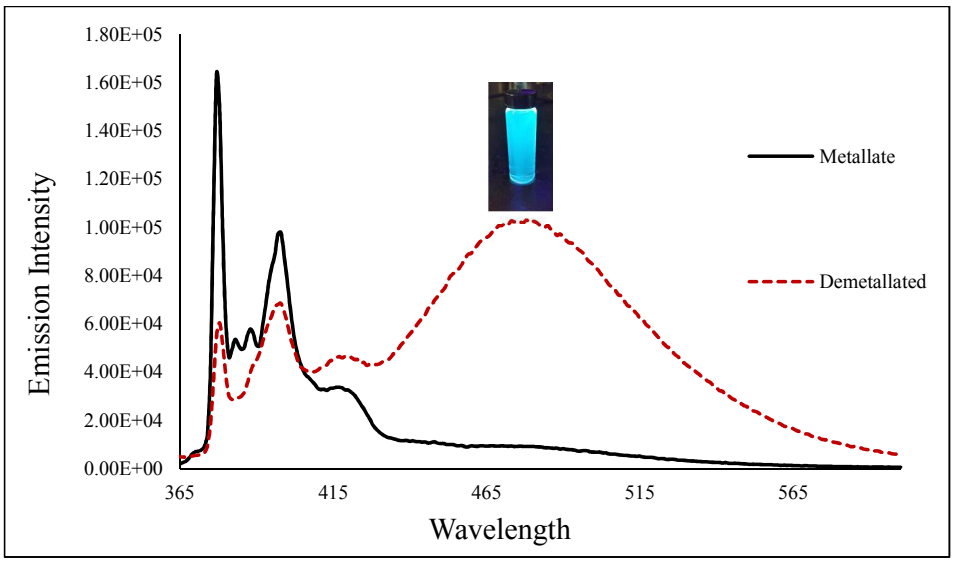

Figure 9. Representative plot of the effect of demetallation on emission intensity of dendrimer **D8** (10μM) and demetallated dendrimer **D9** (10μM) in THF.

The fluorescence spectra of dendrimers **D3a,b, D5, D9,** and **D13** in different solvents such as dimethyl sulfoxide (DMSO), N,N-dimethylformamide (DMF), dichloromethane (DCM), acetonitrile (ACN), chloroform, tetrahydrofuran (THF), and cyclohexane showed typical emission of pyrenyl groups at 377, 398, and 470 nm for demetallated dendrimers **D3a,b, D5,** and **D9**, while for demetallated dendrimer **D13**, the excimer emission was around 480 nm. The plots of the excimer-monomer intensity ratios (I_E/I_M) for the dendrimers **D3a,b, D5, D9,** and **D13** with dielectric constant of the solvents depicted in Figure 10. In low polarity solvents when the dielectric constant (ε_r) was less than 30, (I_E/I_M) values of G0 dendrimers **D3a,b** and **D5,** G1 dendrimer **D9**, and G2 dendrimer **D13** were less than 0.35. However, (I_E/I_M) increase as the ε_r become greater than 30. This is due to the intramolecular or

intermolecular π- stacking interaction due to increasing in solvent polarities. The higher the solvent polarity the greater the ability for the two pyrenyl units to be close to each other to form the excimer. The order of excimer-monomer intensity ratios of the generation was G2 > G1 > G0, which may be due to the impact of the number of pyrenyl groups. Second generation dendrimer **D13** has sixteen chromophoric moieties, but the first generation dendrimer **D9** has eight chromophoric moieties, while dendrimers **D3a,b** and **D5** in the zero generation have only four chromophoric moieties. Also, the different flexible aliphatic chains attached to the dendrimers in the zero generation may contribute to the differences in (I_E/I_M) values in term of intramolecular excimer formation, with the solvent molecules surrounding the dendrimers.

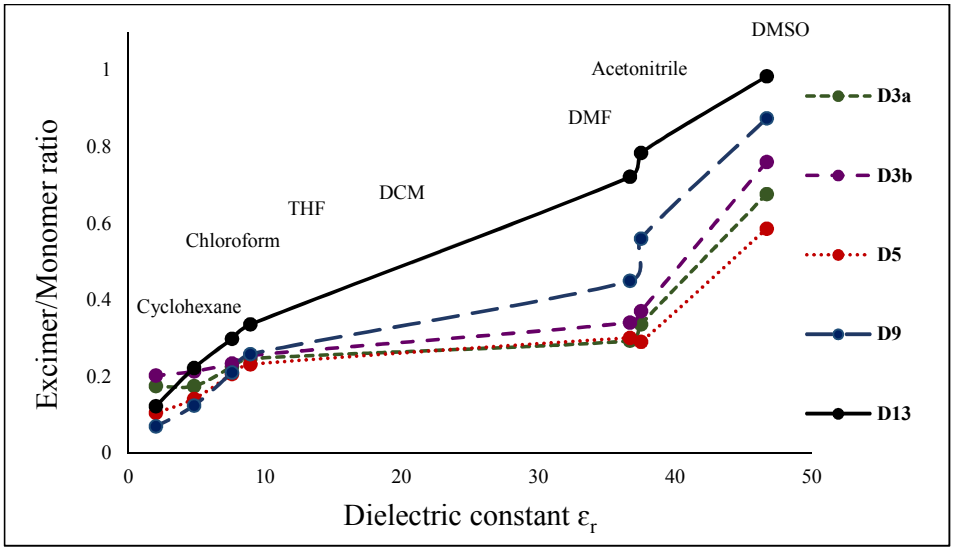

Figure 10. (I_E/I_M) intensity ratios, for dendrimers **D3a,b, D5, D9,** and **D13** and dialectic constant (ε_r) at 100μM, λ_{ex}=343 nm.

Our results suggest that the excimer formation increases with increasing concentration, which agrees with the previous studies, and indicates a significant contribution from intermolecular excimer formation.[37] In the low concentration region 1 μM to 10 μM, in THF of dendrimer **D3a,b, D5, D9,** and **D13** we found a slight increase in the excimer-monomer intensity ratio (I_E/I_M), with increasing concentration, but it reached a maximum at 0.36. The major emission

peaks were located at 377 and 398 nm due to the emission of the monomeric species in the solution. When the concentration was increased to 50 μM, the red-shift excimer peak became strong. This peak provides evidence for the existence of excited state pyrene dimers; however, the monomer did not disappear. The excimer-monomer intensity ratio (I_E/I_M) increased with increasing concentration to 200 μM, and the dendrimers became stronger excimer emitters with increasing concentration. To prove this, we prepared more concentrated solutions, as excimer emission is known to be concentration-dependent. With an increase in the dendrimer concentration, the excimer emission becomes dominant at 400 μM, and the excimer-monomer intensity ratios (I_E/I_M) increased to 2.7. This high differences in the ratio with increasing concentration demonstrate that it originates from pyrene intermolecular interaction pyrene excimers (Figure 11).

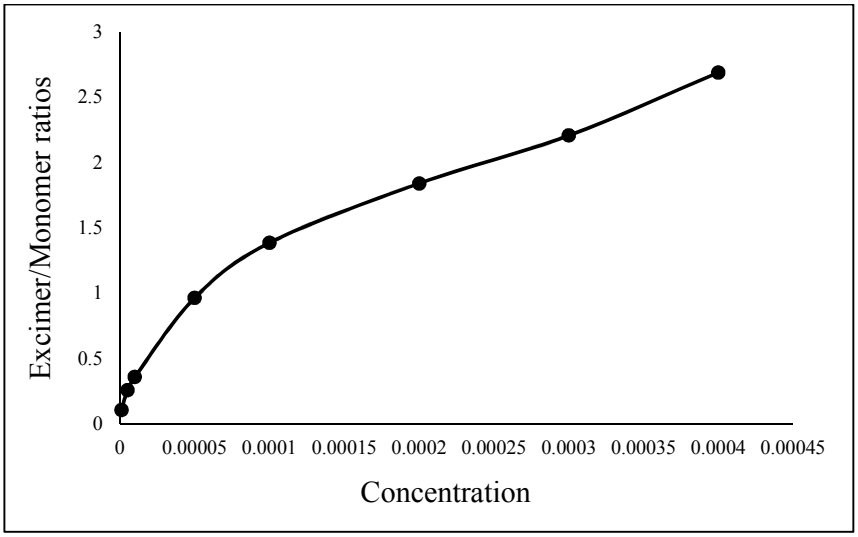

Figure 11. Representative (I_E/I_M) intensity ratios for dendrimer **D3b**, in THF concentration between (1 μM and 400 μM), λ_{ex}=343 nm.

Florescence in the aggregated state

In the next step, we wanted to determine whether dendrimers **D3a,b, D5, D9,** and **D13** were AEEE-active or not. All dendrimers were investigated in mixtures of THF/water. The concentration of the solution was kept constant at 10μM for all dendrimers. A stock solution

of a given dendrimer in THF with a concentration of 100 μM was prepared. Then 1 mL of this stock solution was transferred to 10 mL volumetric flasks. After that, we added an appropriate amount of a THF/water mixture with a specific water fraction (f_w), the water content was varied in range (0-90 vol %). Absorption and emission spectra of the resulting solutions were measured immediately after the samples were prepared. For all measurements, excitation was at 343 nm. We chose the low concentration of 10 μM to avoid excimer formation in a pure organic solvent (THF), and to study the effect of aggregation due to the addition of a poorly solubilizing solvent in enhanced excimer formation, since as mentioned before, not all dendrimers form a high percentage of excimers at low concentration.

All dendrimers displayed distincitive absorption bands at 328 and 343 nm in pure THF and in a THF/water when the fraction of water was less than 80%. When the water fraction was increased to 80 %, the absorption band became weaker and shifted to the longer wavelength at 332 and 349 nm. Due to the dependence of absorption intensity on concentration, more added water caused an increased chance for the particles to aggregate and form solid particles, indicating ground state aggregation was occurring. This leads to a decrease in the concentration, as well as the intensity of the absorption bands (Figure 12).

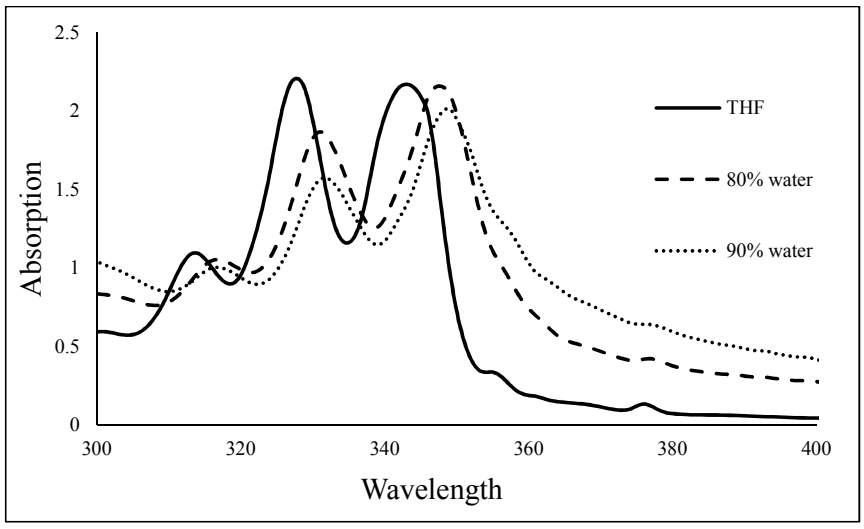

Figure 12. Representative UV-vis absorption spectra of dendrimer **D3a** (10μM) in pure THF and in THF/water mixtures.

Dendrimer **D3a** exhibited prominent emission peaks at 377 and 398 nm in pure THF. These two bands correspond to monomer emission. The intensity of the monomer emission increases slightly as the water percentage increases to 50%. Surprisingly, a red-shift along with an intensity enhancement of the pyrene excimer emission and quenching of the monomer emission resulted in emission at 470 nm when the water percentage was ≥ 60% (Figure 13). At water ≥ 70% the quenching of the pyrene monomer emission increased with more enhancement of the pyrene excimer emission.

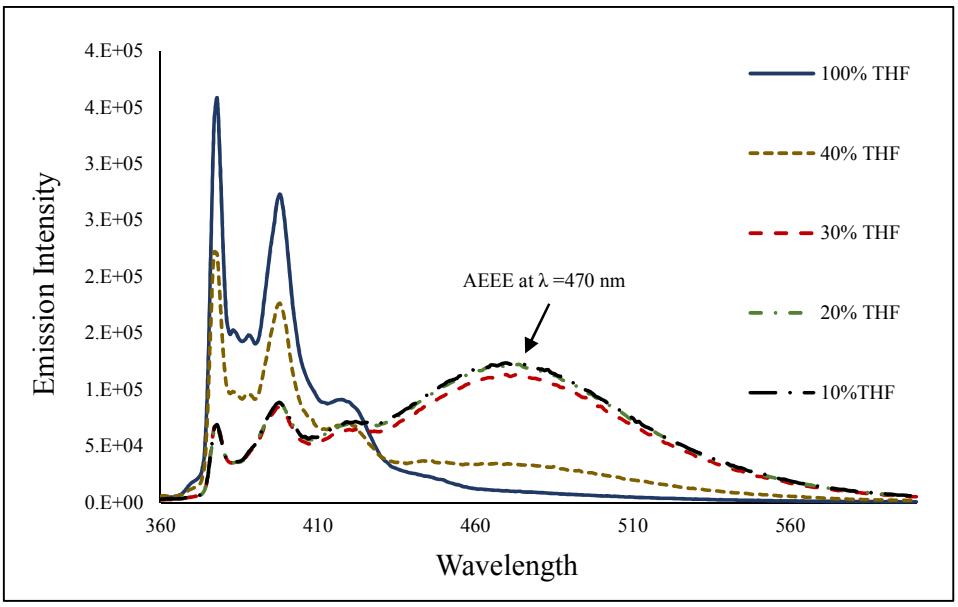

Figure 13. Fluorescence spectra of dendrimer **D3a** (10μM), λ_{ex}= 343 nm in pure THF and upon addition water fraction.

At low fractions of water less than 60%, the distance, or orientation between two pyrene units, was likely not suitable for excimer formation. The presence of alkyl side chains bearing the pyrene fluorescent probe provides more flexibility to the dendrimer as it rotates, and provides an easier path for intra- or intermolecular π-stacking interaction to form the excimer.[30] The increase in the percentage of water results in a decrease in the separation of pyrene molecules in the solution by aggregation. This results in the two neighbor pyrenyl groups coming closer to each other during the rotation to form an excited-state pair.[30]

According to previous studies, there are two types of excimers that depending on the origin of the pyrene dimer; dynamic excimers and static excimers.[33] Dynamic excimer emission is emitted from a pyrene dimer formed in the excited state, whereas static excimer is emission is from a pyrene dimer formed in the ground state. The absorption spectrum of dendrimer **D3a** is similar to the normal pyrene bands at 328 and 343 nm, and the excitation spectrum displays the monomer wavelengths 377 and 398 nm and the excimer emission at 470 nm. These are identical to those recorded, indicating that the emission at 470 nm arises from the dynamic excimer.[31, 34, 58, 59] As the intensity ratio of excimer to monomer emission (I_E/I_M) is sensitive to the distance and conformational changes, we found that the relative ratios when the excimer formed at 60% water were 0.17 and became 1.54 at 90% water (Figure 14). The significant enhancement of the fluorescence intensity at 470 nm is probably due to the intramolecular π-stacking interaction and restriction of intermolecular rotation motion (RIMR) of the pyrenyl groups. Therefore, the fluorescence from intramolecular excimers,[60] can be formed rapidly by the association between adjacent pyrene moieties in the same molecule due to increasing in the solvent polarities. In dendrimer **D3a** in high water fractions, the polarity of the solvent increased and this led to the two pyrenyl units located in the vicinity allow for an intramolecular excimer state to be formed upon excitation. The intramolecular nature of excimer generation, as a result of the steric pattern of pyrenyl units, was suggested by the observation of the significant increase in the excimer-monomer intensity ratio upon increasing the polarity by increasing of water fraction to 70%.[61]

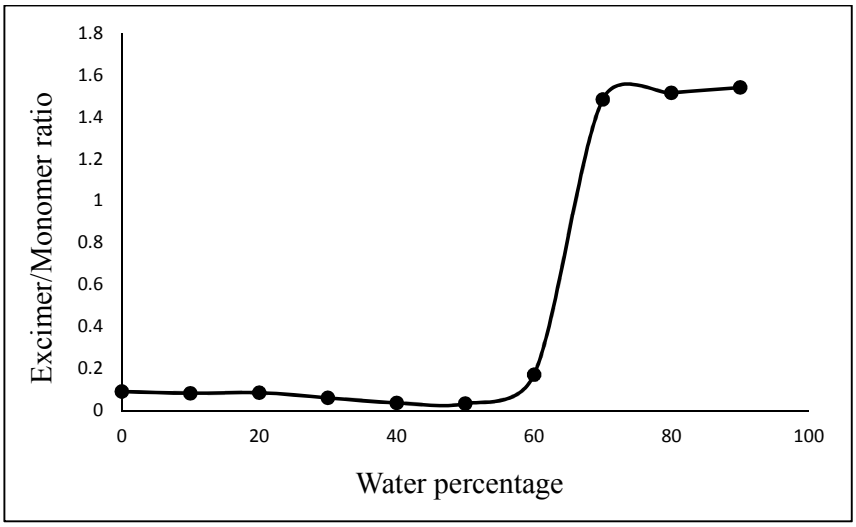

Figure 14. (I_E/I_M) intensity ratios of dendrimer **D3a** (10μM), λ_{ex}= 343 nm in pure THF and upon addition water fraction.

We prepared different five concentrations between (1μM to 100μM) for (1:9 v/v) THF/water solutions, as excimer emission is known to be concentration dependent. With an increase in the concentration, the emission at 470 nm becomes increased, and the excimer-monomer intensity ratios (I_E/I_M) increased from 1.3 at 1μM to 1.7 at 100μM. This enhancement behavior indicated that the excimers were formed by intermolecular π-stacking interaction pyrene (Figure 15). In conclusion, both intra- and intermolecular π-stacking interaction can be observed in dendrimer **D3a**, as a result of changing in solvent polarities or concentration.

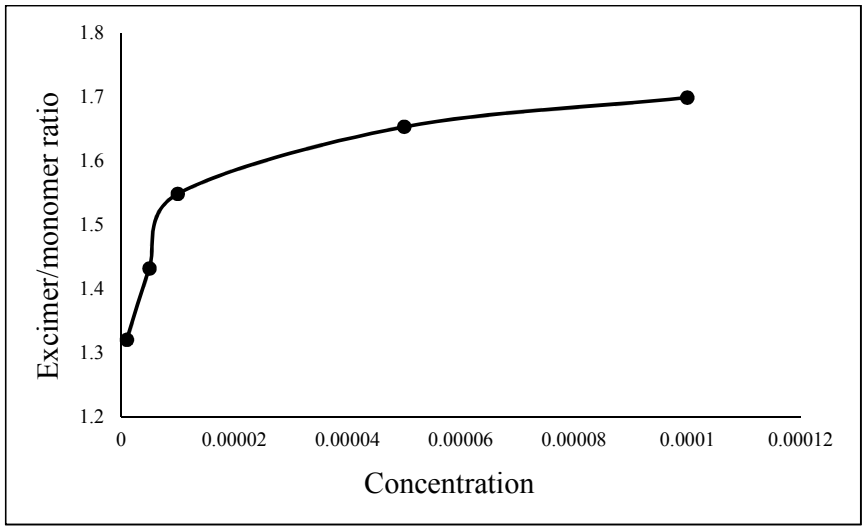

Figure 15. (I_E/I_M) intensity ratios for dendrimer **D3a**, in THF/water (1:9 v/v), in different concentrations between (1 µM and 100 µM), λ_{ex}=343 nm.

The same trend was observed in dendrimer **D3b**, as the consistently increasing water ratios resulted in the emission intensity remaining at the wavelength of the monomeric emission region of pyrene. Almost all of the emission was due to the monomer and no significant excimer emission is observed until f_w equal 60%. The pyrene excimers appeared suddenly at 470 nm in 70% water (Figure 16), and the ratio I_E/I_M, increases with the increasing in water percentage.

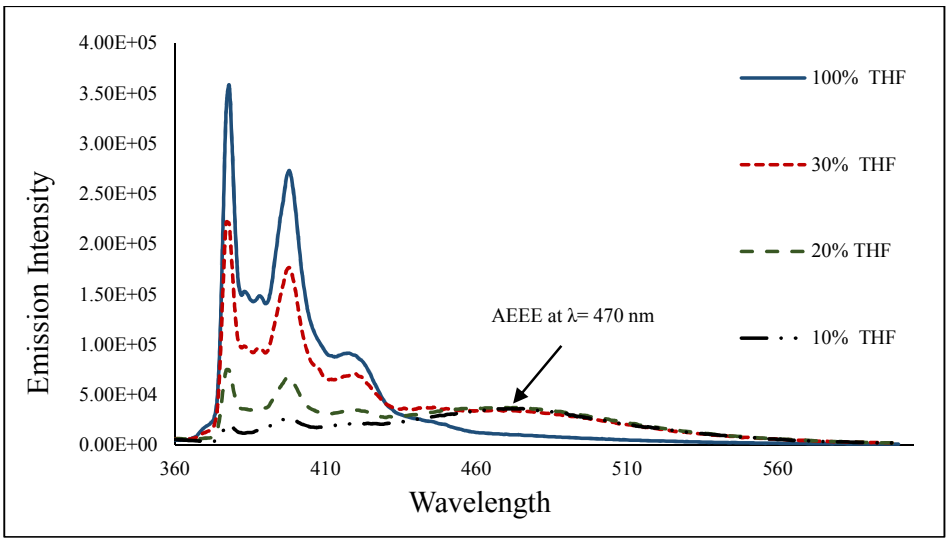

Figure 16. Fluorescence spectra of dendrimer **D3b** (10µM), λ_{ex}= 343 nm in pure THF and upon addition water fraction.

The only difference between dendrimer **D3a** and **D3b** is that the excimer formed in dendrimer **D3a** at 60% water. The excimer-monomer intensity ratio stays constant at around 1.5 as the water fraction is increased from 70 to 90%. In contrast, although the excimer formed in dendrimer **D3b** at higher water fraction than dendrimer **D3a**, (started to appear at 70% water), the ratio between excimer and monomer emission showed a dramatic increase between 70 and 90%, with values of 0.17, 0.49, and 1.2 for 70, 80 and 90% of water, respectively (Figure 17). The flexibility of the long chain may impact the excimer formation. In dendrimer **D3a** (containing eight carbons in this chain), the aggregation by addition of more water made two pyrene molecules come together more efficiently than in dendrimer **D3b** (twelve carbons). Also, the more flexible dendrimer **D3b** needs to be more aggregated and closer to each other to form the excimer. This happened when the water fraction was increased to 90%. In the less flexible dendrimer **D3a**, the two pyrene molecules were already at a suitable distance to aggregate and the increasing water percentage from 70-90% had a negligible effect.

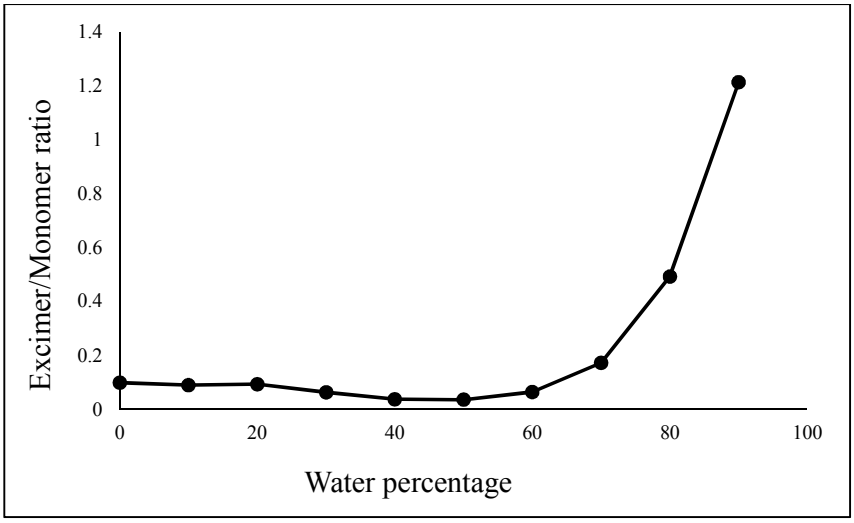

Figure 17. (I_E/I_M) intensity ratios of dendrimer **D3b** (10μM), λ_{ex}= 343 nm in pure THF and upon addition water fraction.

When dendrimer **D5** was excited at 343 nm, the spectrum displayed monomer emissions at 377 and 398, and excimer emission at 470 nm. Aggregation enhanced excimer emission (AEEE) with quenched monomer emission were observed, as the new aggregation-induced excimer emission occurs in the blue region of the visible spectrum, in contrast to the monomer emission which occurs in the UVA region. Thus, an intense blue emission appears upon aggregation (AEEE). The excimer-monomer intensity ratios moderately increased with increasing water fraction (Figure 18).

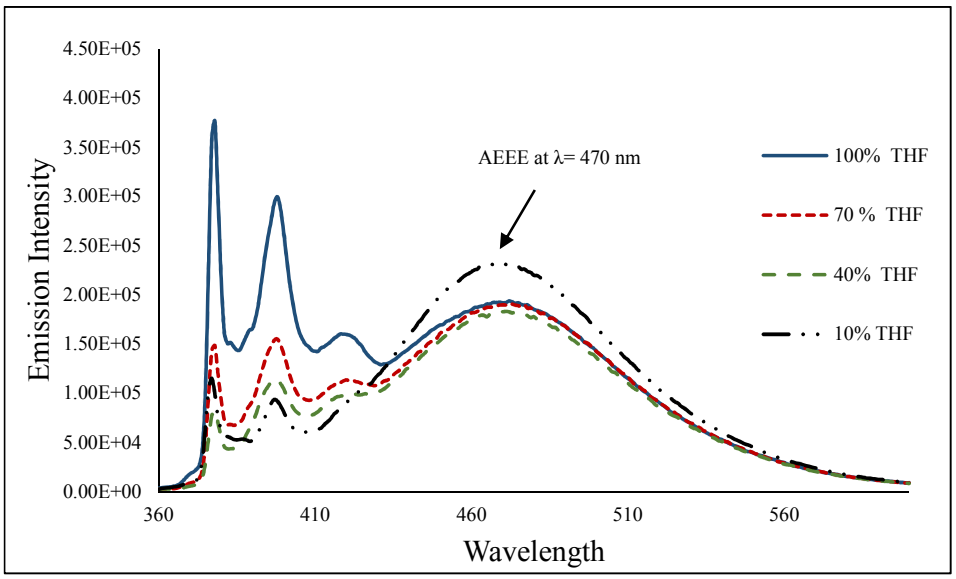

Figure 18. Fluorescence spectra of dendrimer **D5** (10μM), λ_{ex}=343 nm in pure THF and upon addition water fraction.

This is different from the spectra observed in dendrimers **D3a** and **D3b** as in the case of dendrimer **D5** the pyrene is attached directly to the zero generation without flexible chain. The monomer emission band should be attributed to the individual pyrene moieties in the isolated state while the red-shifted band approaching 470 nm should be attributed to the pyrene aggregates or excimers. This might be related to the presence of pyrene molecules being in close proximity to induce inter- or intramolecular π-stacking interaction excimers, which causes long-wavelength emission. However, the intensity of the excimer band varied

depending on the distance between pyrene moieties,[62] and it is clearly observed that the (I_E/I_M) intensity ratio significantly increases with increasing water percentage. The values were 0.54 in pure THF and 2.66 in the 1:9 THF/water mixture. This suggests that the excimer emission is due to intramolecular interactions in high water fraction due to aggregation by increasing the solvent polarity (Figure 19).

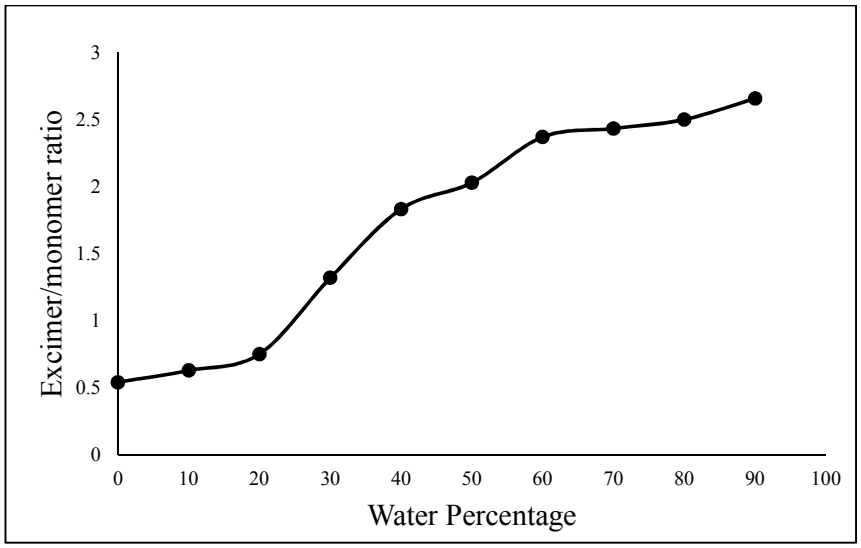

Figure 19. (I_E/I_M) intensity ratios of dendrimer **D5** (10μM), λ_{ex}= 343 nm in pure THF and upon addition water fraction.

In dendrimer **D9,** twice the number of pyrenyl groups decorate the periphery of this first generation. The excitation at 343 nm showed monomer emission at wavelength 377 and 398 nm while excimer formation was recorded at 470 nm. Indeed, in high water fractions started at 70% the excimer emission was red-shifted relative to that in the case of the lower water fractions which had a wavelength maximum of 480 nm. This could be a result of the decreasing distance between the two pyrene groups due to the presence of more water fractions (70-90%) (Figure 20).

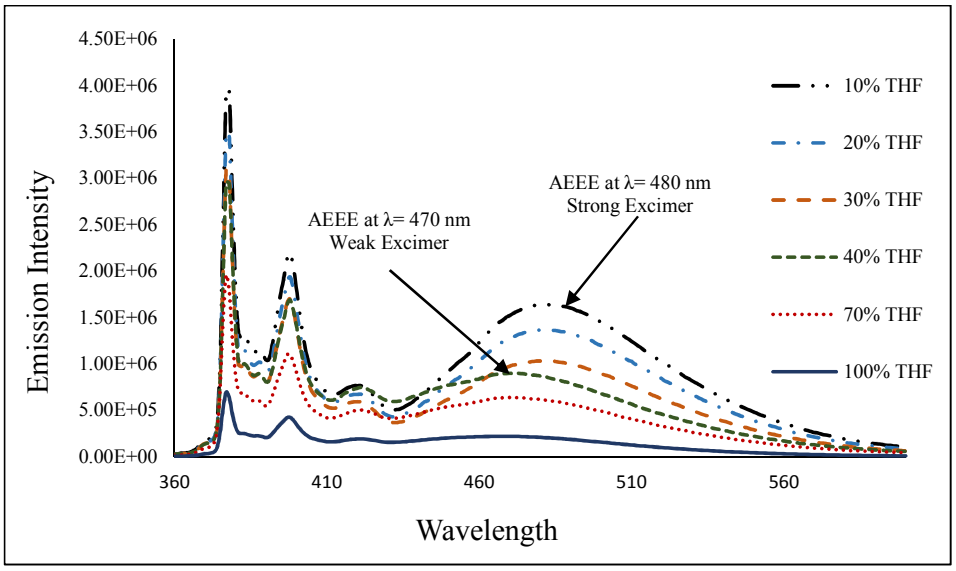

Figure 20. Fluorescence spectra of dendrimer **D9** (10μM), λ_{ex}= 343 nm in pure THF and upon addition water fraction.

The monomer and excimer emission were enhanced together in all water fractions but with a slight increase in the excimer-monomer intensity ratios from 0.4 to 0.47, up to 60% water. At water ≥ 70% the excimer formation enhanced more than the monomer, this is very clear from the increasing of the excimer-monomer intensity ratios from 0.47 at 60% water to 0.74 at 90% water. The overall increasing of the excimer-monomer intensity ratios from 0.4 in pure THF to 0.74 in 1:9 THF/water supports the self-assembled intramolecular π-stacking of pyrenyl rings (Figure 21). The pyrenyl groups in dendrimer **D9** exist in close proximity, allowing an intramolecular excimer state to be reached upon excitation. Thus, we can conclude that this red-shift in the wavelength is due to the shorter distance between two pyrene moieties by aggregation which leads to strong excimer formation and might also cause intermolecular interaction between different molecules.[61, 62]

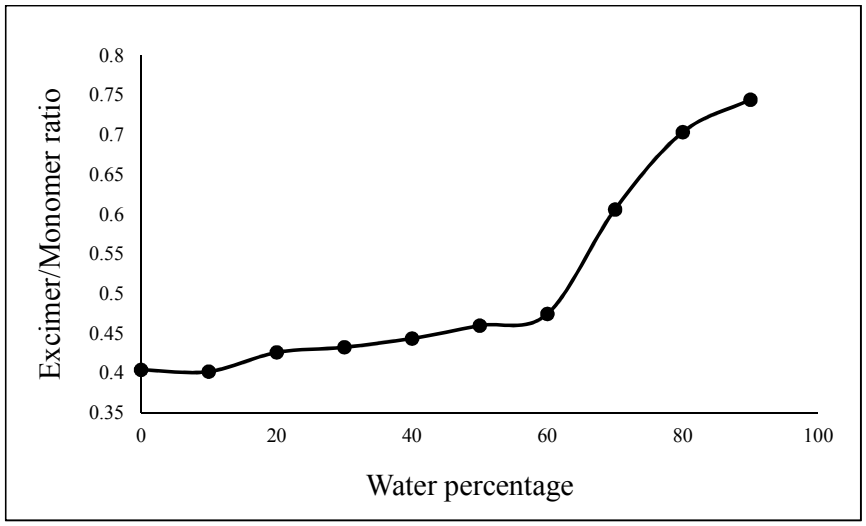

Figure 21. (I_E/I_M) intensity ratios of dendrimer **D9** (10μM), λ_{ex}= 343 nm in pure THF and upon addition water fraction.

Aggregation Enhanced Excimer Emission (AEEE) as also observed in the second generation dendrimer **D13,** which showed the same trends relative to dendrimer **D5** upon excitation at 343 nm. At various water fractions, the two emission peaks for the monomer emission appeared at 377 and 398 nm, while the excimer emission appeared at 480 nm. The excimer emission appeared at 480 nm which indicated strong excimer formation which may be due to the high number of pyrene moieties in the dendrimer periphery relative to the zero and first generation. The quenching of the monomer emission with enhancement of the excimer emission occurred from the first adding of water up to 90% water (Figure 22).

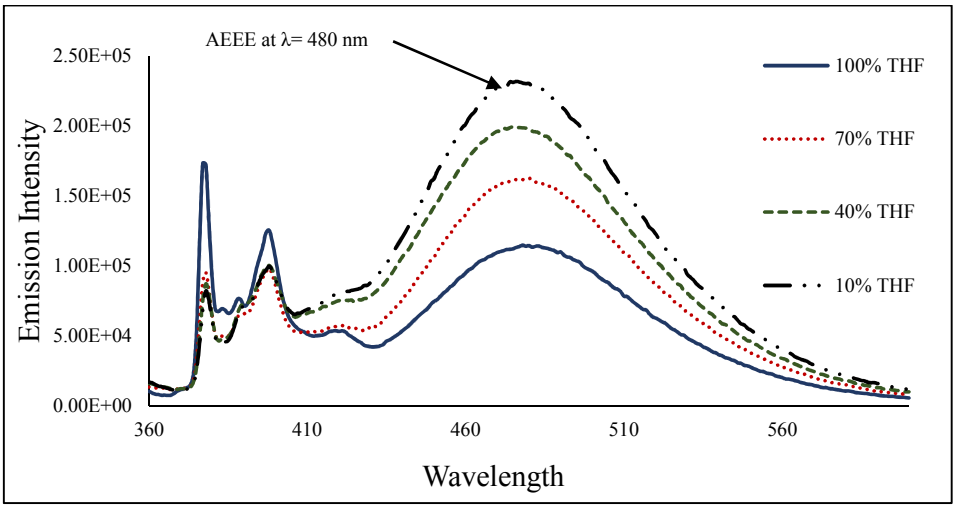

Figure 22. Fluorescence spectra of dendrimer **D13** (10μM), λ_{ex}= 343 nm in pure THF and upon addition water fraction.

The (I_E/I_M) intensity ratio shows a significant increase with increasing water fraction (Figure 23). The formation of strong excimer at 480 nm, and increasing of the excimer-monomer intensity ratios were observed, which made both inter- and intramolecular interaction possible due to the high numbers of pyrene moieties in the periphery of the **D13** relative to **D3a**,**d**, **D5**, and **D9** in the zero and first generation.

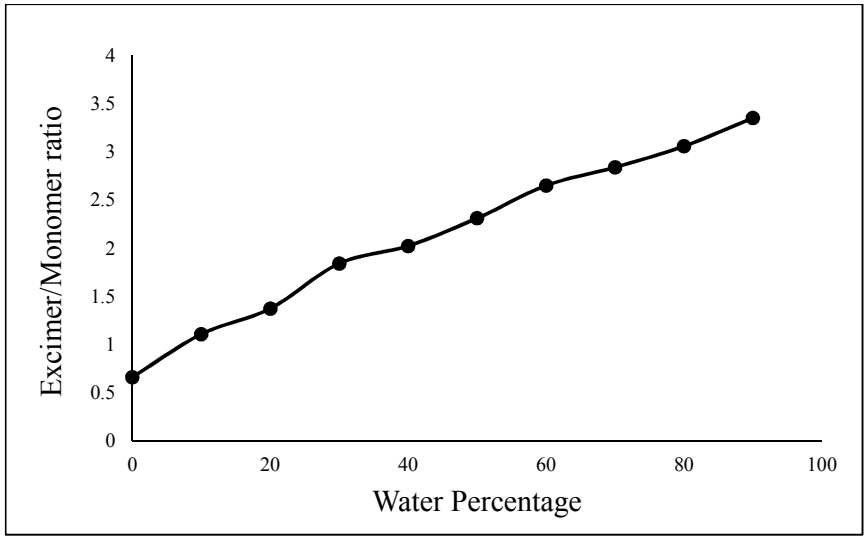

Figure 23. (I_E/I_M) intensity ratios of dendrimer **D13** (10μM), λ_{ex}= 343 nm in pure THF and upon addition water fraction.

The transmission electron microscope image (TEM) of the aggregate structure of representative dendrimer **D3a** in pure THF and a THF/water mixture were observed as shown in Figure 24. A 10 microliter sample was placed on a carbon-coated copper grid. The sample was suspended in either THF, which evaporated immediately, or a THF/water mixture left for 30 seconds on the grid and blotted with filter paper. The effect of aggregation on size, shape, and distribution was investigated and showed hugely different images in each THF/water fraction. In pure THF, the molecules appear as a large number of separated spherical particles (Figure 24-a). The size of these spherical particles is between 400 and 900 nm. However, by the addition of water fraction the particles became smaller, and with 20% water, the particles' sizes are between 165 and 600 nm (Figure 24-b). Nanoparticles started to appear at 40% water, with well-defined spherical shapes. Also, it can be definitely seen that all these particles are well joined to each other (Figure 24-c). The existence of nanodimensional aggregates predominates in 60% water, and the average size is 50 nm (Figure 24-d). In 80% water, the results were markedly different, in that the spherical shape started to disappear and a small number of the particles remained in nanoparticle spherical shape and aggregated together (Figure 24-e). TEM for the 90% water is totally different, the spherical particles disappeared and the shape looks like leaves which indicated a more aggregated structure (Figure 24-f). This was likely due to the high degree of steric crowding by aggregation due to the presence of a poor solvent.

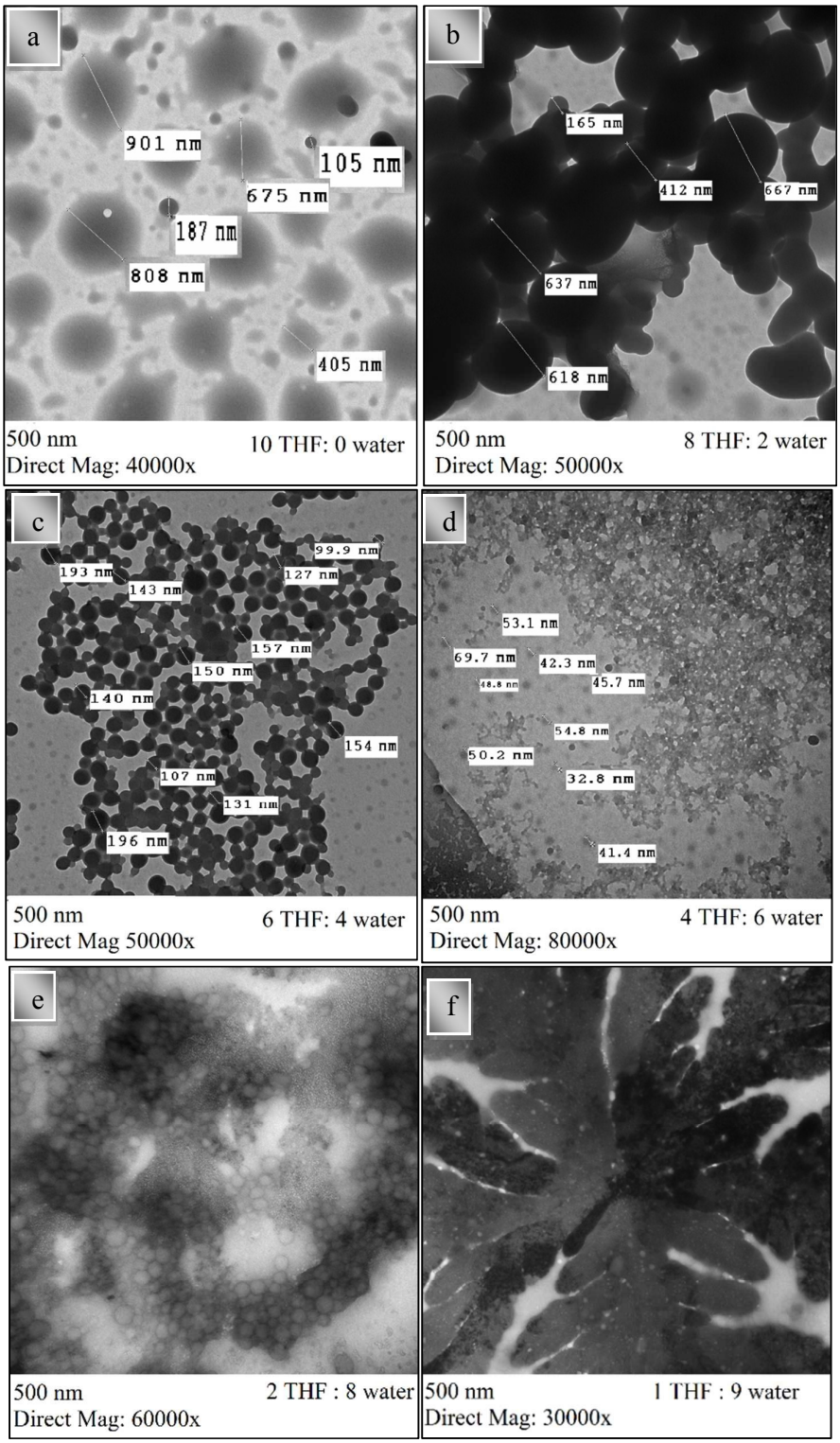

Figure 24. Transmission electron microscope images (TEM) for dendrimer **D3a** in different THF/water mixtures.

4. Conclusions

In summary, the highlights of the present study are synthesis and characterization of a novel set of dendrimers peripherally modified by pyrene units. A unique red-shift along with fluorescent enhancement in pyrene excimer emission was observed, which was induced by the formation of dynamic pyrene excimers. The aggregation increased the excimer formation efficiency of dendrimers **D3a** and **D3b** due to the intramolecular π-stacking interaction between two pyrenyl rings in high water fractions. In addition, we have shown here strong and weak excimer formation by intra and/or intermolecular interactions, in dendrimers **D9** and **D13**, with simple aggregation enhanced excimer emission (AEEE). The quenching of monomer emission with enhancement of excimer emission was observed very clearly in dendrimer **D5** and **D13**. In particular, **D13** showed red-shift emission relative to the other dendrimers and intensity enhancement of the pyrene excimer-monomer ratio (I_E/I_M) by increasing water fraction. The emissions depend on the dielectric constant of the solvents as well as concentration. This type of AEEE-active dendrimers is expected to be applied in the field of photoactive dendrimers in the future.

Acknowledgments

Support from NSERC and CFI is gratefully appreciated. Dr. Elsayed. M. Abdelrehim of the Faculty of Science, University of Damanhour and Ms. Amani Abdelghani of the Faculty of Science, Damanhour University would like to express their gratitude to the Egyptian mission sector, Damanhour University and Alexandria University for their support. A.A is also grateful to Dr. Samir K. Elsadany, Dr. Mohamed K. Awad and Dr. Ezzat A. Hamed for their invaluable advice.

References

1. Hecht, S.; Fréchet, J. M. *Angew. Chem. Int. Ed. Engl.* 2001, **40**, 74-91.

2. Tomalia, D. A.; Baker, H.; Dewald, J.; Hall, M.; Kallos, G.; Martin, S.; Roeck, J.; Ryder, J.; Smith, P. *Polym. J.* 1985, **17**, 117-132.

3. Newkome, G. R.; Yao, Z.; Baker, G. R.; Gupta, V. K. *J. Org. Chem*. 1985, **50**, 2003-2004.

4. Alonso, B.; Moran, M.; Casado, C. M.; Lobete, F.; Losada, J.; Cuadrado, I. *Chem. Mater.* 1995, **7**, 1440-1442.

5. Liu, M.; Fréchet, J. M. Pharm. *Sci. Tech. Today* 1999, **2**, 393-401.

6. Svenson, S.; Tomalia, D. A. *Adv. Drug Deliv. Rev*. 2005, **57**, 2106-2129.

7. Hawker, C.; Fréchet, J. M. Journal of the ***J. Chem. Soc., Chem. Commun.*** 1990, 1010-1013.

8. Hawker, C. J.; Fréchet, J. M. *J. Am. Chem. Soc.* 1990, **112**, 7638-7647.

9. Gorman, C. B.; Parkhurst, B. L.; Su, W. Y.; Chen, K. *J. Am. Chem. Soc.* 1997, **119**, 1141-1142.

10. Newkome, G. R.; Güther, R.; Moorefield, C. N.; Cardullo, F.; Echegoyen, L.; Pérez-Cordero, E.; Luftmann, H. *Angew. Chem. Int. Ed. Engl.* 1995, **34**, 2023-2026.

11. Liao, Y.; Moss, J. R. *Organometallics.* 1996, **15**, 4307-4316.

12. Abd-El-Aziz, A. S.; Agatemor, C.; Etkin, N.; Bissessur, R. *Macromol. Chem. Phys.* 2015, **216**, 369-379.

13. Cuadrado, I.; Morán, M.; Casado, C. M.; Alonso, B.; Losada, *J. Coord. Chem. Rev.* 1999, **193**, 395-445.

14. Lauher, J. W.; Hoffmann, R. *J. Am. Chem. Soc.* 1976, **98**, 1729-1742.

15. Lauher, J. W.; Elian, M.; Summerville, R. H.; Hoffmann, R. *J. Am. Chem. Soc.* 1976, **98**, 3219-3224.

16. Astruc, D. *New J. Chem.* 2009, **33**, 1191-1206.

17. Djeda, R.; Ornelas, C.; Ruiz, J.; Astruc, D. *Inorg. Chem.* 2010, **49**, 6085-6101.

18. Juris, A. *Ann. Rep. Progr. Chem.* 2003, **99**, 177-241.

19. Abd-El-Aziz, A. S.; Todd, E. K.; Okasha, R. M.; Shipman, P. O.; Wood, T. E. *Macromolecules* 2005, **38**, 9411-9419.

20. Abd-El-Aziz, A. S.; Strohm, E. A.; Ding, M.; Okasha, R. M.; Afifi, T. H.; Sezgin, S.; Shipley, P. R. *J Inorg Organomet Polym Mater.* 2010, **20**, 592-603.

21. Abd-El-Aziz, A. S.; Carruthers, S. A.; Aguiar, P. M.; Kroeker, S. *J Inorg Organomet Polym Mater.* 2005, **3**, 349-359.

22. Abruña, H. D. *Anal. Chem.* 2004, **76**, 310 A-319 A.

23. Boubbou, K. H.; Ghaddar, T. H. *Langmuir* 2005, **21**, 8844-8851.

24. Venturi, M.; Serroni, S.; Juris, A.; Campagna, S.; Balzani, V. Dendrimers; *Springer*, 1998, **197**, 193-228.

25. Vögtle, F.; Plevoets, M.; Nieger, M.; Azzellini, G. C.; Credi, A.; De Cola, L.; De Marchis, V.; Venturi, M.; Balzani, V. *J. Am. Chem. Soc.* 1999, **121**, 6290-6298.

26. Kondo, S.; Taguchi, Y.; Bie, Y. *RSC Advances.* 2015, **5**, 5846-5849.

27. Haedler, A. T.; Misslitz, H.; Buehlmeyer, C.; Albuquerque, R. Q.; Köhler, A.; Schmidt, H. *Chem. Phys Chem.* 2013, **14**, 1818-1829.

28. Chou, T.; Hwa, C.; Lin, J.; Liao, K.; Tseng, J. *J. Org. Chem.* 2005, **70**, 9717-9726.

29. Nandy, R.; Subramoni, M.; Varghese, B.; Sankararaman, S. *J. Org. Chem.* 2007, **72**, 938-944.

30. Dabestani, R.; Kidder, M.; Buchanan Iii, A. *J. Phys. Chem. C.* 2008, **112**, 11468-11475.

31. Yang, J.; Lin, C.; Hwang, C. *Org. Lett.* 2001, **3**, 889-892.

32. Birks, J.; Dyson, D.; Munro, I. *Proc. R. Soc. A*, 1963, **275**, 1363.

33. Winnik, F. M. *Chem. Rev*. 1993, **93**, 587-614.

34. Ghosh, A.; Sengupta, A.; Chattopadhyay, A.; Das, D. *Chem. Commun.* 2015, **51**, 11455-11458.

35. Yuan, W. Z.; Gong, Y.; Chen, S.; Shen, X. Y.; Lam, J. W.; Lu, P.; Lu, Y.; Wang, Z.; Hu, R.; Xie, N. *J. Chem. Mater.* 2012, **24**, 1518-1528.

36. Aldred, M. P.; Li, C.; Zhang, G.; Gong, W.; Li, A. D.; Dai, Y.; Ma, D.; Zhu, M. *J. Mater. Chem.* 2012, **22**, 7515-7528.

37. Luo, J.; Xie, Z.; Lam, J. W.; Cheng, L.; Chen, H.; Qiu, C.; Kwok, H. S.; Zhan, X.; Liu, Y.; Zhu, D. *J. Chem. Commun.* 2001, 1740-1741.

38. Tang, B. Z.; Lee, P. P. *J. Chem. Mater*. 2001, **11**, 2974-2978.

39. Watson, M. D.; Jäckel, F.; Severin, N.; Rabe, J. P.; Müllen, K. *J. Am. Chem. Soc.* 2004, **126**, 1402-1407.

40. Nandy, R.; Subramoni, M.; Varghese, B.; Sankararaman, S. *J. Org. Chem. 2007,* **72**, 938-944.

41. Sankararaman, S.; Venkataramana, G.; Varghese, B. *J. Org. Chem*. 2008, **73**, 2404-2407.

42. Kimura, M.; Miki, N.; Suzuki, D.; Adachi, N.; Tatewaki, Y.; Shirai, H. *Langmuir* 2008, **25**, 776-780.

43. Issberner, J.; Vögtle, F.; Cola, L. D.; Balzani, V. *Chem. Eur. J.* 1997, **3**, 706-712.

44. Archut, A.; Vögtle, F.; De Cola, L.; Azzellini, G. C.; Balzani, V.; Ramanujam, P.; Berg, R. H. *Chem. Eur. J.* 1998, **4**, 699-706.

45. Abd-El-Aziz, A. S.; Carruthers, S. A.; Todd, E. K.; Afifi, T. H.; Gavina, *J. Polym. Sci. A Polym. Chem.* 2005, **43**, 1382-1396.

46. Abd-El-Aziz, A.; May, L.; Hurd, J.; Okasha, R. *J. Polym. Sci. A Polym. Chem.* 2001, **39**, 2716-2722.

47. Neises, B.; Steglich, W. *Angew. Chem. Int. Ed. Engl.* 1978, **17**, 522-524

48. Abd-Ei-Aziz, A. S.; Armstrong, D. A.; Bernardin, S.; Hutton, H. M. *Can. J. Chem* 1996, **74**, 2073-2082.

49. Wang, Y.; Rapakousiou, A.; Astruc, D. *Macromolecules* 2014, **47**, 3767-3774.

50. Balzani, V.; Campagna, S.; Denti, G.; Juris, A.; Serroni, S.; Venturi, M. *Acc. Chem. Res.* 1998, **31**, 26-34.

51. Astruc, D. *Nat. Chem.* 2012, **4**, 255-267.

52. Abd-El-Aziz, A. S.; Agatemor, C.; Etkin, N. *Macromol. Rapid Commun.* 2014, **35**, 513-559.

53. Edwards, E.; Antunes, E.; Botelho, E. C.; Baldan, M.; Corat, E. *Appl. Surf. Sci.* 2011, **2**, 641-648.

54. Albrecht, K.; Yamamoto, K. *J. Am. Chem. Soc.* 2009, **131**, 2244-2251.

55. Li, Y.; Han, L.; Chen, J.; Zheng, S.; Zen, Y.; Li, Y.; Li, S.; Yang, G. *Macromolecules* 2007, **40**, 9384-9390.

56. Bodenant, B.; Fages, F.; Delville, M. *J. Am. Chem. Soc.* 1998, **120**, 7511-7519.

57. Sahoo, D.; Narayanaswami, V.; Kay, C. M.; Ryan, R. O. *Biochemistry (N.Y.)* 2000, **39**, 6594-6601.

58. Jun, E. J.; Won, H. N.; Kim, J. S.; Lee, K.; Yoon, *J. Tetrahedron Lett.* 2006, **47**, 4577-4580.

59. Kim, S. K.; Bok, J. H.; Bartsch, R. A.; Lee, J. Y.; Kim, *J. S. Org. Lett.* 2005, **7**, 4839-4842.

60. Yang, R.; Chan, W.; Lee, A. W.; Xia, P.; Zhang, H.; Ke'An L i*, *J. Am. Chem. Soc.* 2003, **125**, 2884-2885.

61. Lee, S. H.; Kim, S. H.; Kim, S. K.; Jung, J. H.; Kim, *J. S. J. Org. Chem.* 2005, **70**, 9288-9295.

62. Bains, G. K.; Kim, S. H.; Sorin, E. J.; Narayanaswami, V. *Biochemistry (N.Y.)* 2012, **51**, 6207-6219.

Aggregation Enhanced Excimer Emission (AEEE) with Efficient Blue Emission Based on Pyrene Dendrimers

A series of fluorescence dendrimers with terminal pyrene moieties was prepared. The dendrimers exhibited aggregation enhanced excimer emission (AEEE) when water was added to the THF solutions. Changes in the dendrimer generation from zero to two resulted in an increase in the number of the pyrene moieties, which caused much bluer light emitted at 480 nm with a high excimer-monomer emission intensity ratio (I_E/I_M).